Dental pulp of the third molar: a new source of pluripotent-like stem cells

Maher Atari[1,2], Carlos Gil-Recio[1], Marc Fabregat[1], Dani García-Fernández[1], Miguel Barajas[3], Miguel A. Carrasco[4], Han-Sung Jung[5], F. Hernández Alfaro[2], Nuria Casals[6], Felipe Prosper[3], Eduard Ferrés-Padró[2] and Luis Giner[1,2,*]

[1]Laboratory for Regenerative Medicine, College of Dentistry, Universitat Internacional de Catalunya, Barcelona 08009, Spain
[2]Surgery and Oral Implantology Department, College of Dentistry, Universitat Internacional de Catalunya, Barcelona 8017, Spain
[3]Area of Haematology, University of Navarra, Pamplona 31008, Spain
[4]Area of Pathology Universitat Internacional de Catalunya, Barcelona 08195, Spain
[5]Division in Anatomy and Developmental Biology, Department of Oral Biology, Oral Science Research Center, College of Dentistry, Yonsei University, Seoul 120-749, South Korea
[6]Basic Sciences Department and CIBER Physiopathology of the Obesity and Nutrition (CIBEROBN), Faculty of Medicine and Health Sciences, Universitat Internacional de Catalunya, Barcelona 08195, Spain

*Author for correspondence (lginer@csc.uic.es, drmaher1972@csc.uic.es)

Accepted 13 February 2012
Journal of Cell Science 125, 3343–3356

doi: 10.1242/jcs.096537

Summary

Dental pulp is particularly interesting in regenerative medicine because of the accessibility and differentiation potential of the tissue. Dental pulp has an early developmental origin with multi-lineage differentiation potential as a result of its development during childhood and adolescence. However, no study has previously identified the presence of stem cell populations with embryonic-like phenotypes in human dental pulp from the third molar. In the present work, we describe a new population of dental pulp pluripotent-like stem cells (DPPSCs) that were isolated by culture in medium containing LIF, EGF and PDGF. These cells are SSEA4$^+$, OCT3/4$^+$, NANOG$^+$, SOX2$^+$, LIN28$^+$, CD13$^+$, CD105$^+$, CD34$^-$, CD45$^-$, CD90$^+$, CD29$^+$, CD73$^+$, STRO1$^+$ and CD146$^-$, and they show genetic stability in vitro based on genomic analysis with a newly described CGH technique. Interestingly, DPPSCs were able to form both embryoid-body-like structures (EBs) in vitro and teratoma-like structures that contained tissues derived from all three embryonic germ layers when injected in nude mice. We examined the capacity of DPPSCs to differentiate in vitro into tissues that have similar characteristics to mesoderm, endoderm and ectoderm layers in both 2D and 3D cultures. We performed a comparative RT-PCR analysis of *GATA4*, *GATA6*, *MIXL1*, *NANOG*, *OCT3/4*, *SOX1* and *SOX2* to determine the degree of similarity between DPPSCs, EBs and human induced pluripotent stem cells (hIPSCs). Our analysis revealed that DPPSCs, hIPSC and EBs have the same gene expression profile. Because DPPSCs can be derived from healthy human molars from patients of different sexes and ages, they represent an easily accessible source of stem cells, which opens a range of new possibilities for regenerative medicine.

Key words: Dental pulp, DPPSC, Pluripotency, Teratoma formation, Embryonic markers, CGH technique

Introduction

Stem cells have the ability to self-renew and to generate mature, differentiated cells (Fuchs and Segre, 2000). The main postnatal function of stem cells is to repair and regenerate the tissues in which they reside. As pluripotent stem cells have become a major focus of scientific research, many techniques have been developed to determine the actual pluripotency of embryonic stem (ES) cells or induced pluripotent stem (iPS) cells. The pluripotency of human stem cells can be tested in two different ways: teratoma formation by cells injected subcutaneously and the aggregation and generation of embryoid bodies (EBs) from cells cultured in vitro (O'Connor et al., 2008; Papapetrou et al., 2009). These techniques demonstrate a multilineage differentiation capability by which stem cells can give rise to cells of all three germ layers (Itskovitz-Eldor et al., 2000; Martin and Evans, 1975).

Dental pulp tissue is thought to be derived from migratory neural crest cells during development (Peters and Balling, 1999; Thesleff and Aberg, 1999), and it has been shown to harbour various populations of multipotent stem/progenitor cells (Miura et al., 2003; Nosrat et al., 2001). To date, multiple human dental stem/progenitor cells have been isolated, characterised, and classified as a group designated 'dental pulp stem cells' (DPSCs). These include stem cells from exfoliated deciduous teeth (SHEDs), periodontal ligament stem cells (PDLSCs), dental follicle progenitor cells (DFPCs) and stem cells from apical papilla (SCAPs). These post-natal populations have mesenchymal stem cell (MSC)-like qualities, namely the capacity for self-renewal, the potential to differentiate into multiple lineages, including osteoblasts and chondroblasts, and a potential for in vitro differentiation into cell types from various embryonic layers, including adipose, bone, endothelial and neural-like tissues (Arthur et al., 2008; Cheng et al., 2008; Cordeiro et al., 2008; Fujii et al., 2008; Gay et al., 2007; Harada et al., 1999; He et al., 2009; Honda et al., 2008; Huo et al., 2010). Many researchers have proposed that DPMSCs are promising candidates for the repair and regeneration of a variety of mesenchymal tissues, such as bone, cartilage and muscle (Dezawa et al., 2005; Noël et al., 2002). These findings, together with those of other studies, also suggest

Journal of Cell Science

that cells from the dental pulp may represent a unique population based on their regenerative potential (About et al., 2000; Gronthos et al., 2000; Iohara et al., 2004; Mina and Braut, 2004; Zhang et al., 2005). However, no optimal culture medium that allows adult stem cell amplification without self-differentiation has yet been reported (d'Aquino et al., 2007; Stevens et al., 2008).

No previous study to date has described the presence and isolation of human dental pulp stem cells with pluripotent-like characteristics at a single-cell level, nor the use of culture media containing LIF (leukaemia inhibitor factor), EGF (epidermal growth factor) and PDGF (platelet derived growth factor) for isolation of these cells. In the present study, we describe the isolation and identification of a subpopulation of pluripotent-like stem cells from the dental pulp of third molars (termed DPPSCs) that show greater regenerative power than currently used mesenchymal stem cells. These DPPSCs are SSEA4$^+$, OCT4$^+$, NANOG$^+$, SOX2$^+$, LIN28$^+$, CD13$^+$, CD105$^+$, CD34$^-$, CD45$^-$, CD90$^+$, CD29$^+$, CD73$^-$, STRO1$^+$ and CD146$^-$. We investigated the capacity of DPPSCs to differentiate in vitro into tissues that have similar characteristics to embryonic mesoderm, endoderm and ectoderm layers in 2D and 3D, as well as their ability to generate EB-like structures and to develop teratoma-like structures when injected into nude mice. We also performed a comparative analysis of GATA4, GATA6, MIXL1, NANOG, OCT3/4, SOX1 and SOX2 by RT-PCR to determine the degree of similarity between DPPSCs, EBs and human iPS cells. DPPSCs are derived from an easily accessible source, and they can be used in future protocols for the regeneration of tissues from the three embryonic layers.

Results

Characterisation and isolation of dental pulp pluripotent stem cells

These studies were carried out with the goal of isolating and purifying a population of pluripotent-like stem cells derived from dental pulp (DPPSCs). We analysed the phenotypes of all populations, each of which corresponds to a dental pulp donor, cultivated at a density of 80−100 cells per cm^2 and expanded at different passages when the cultures reached 60% confluence. Colony formation was observed, especially when the cells were cultured by the hanging drop method. When colonies were seeded into adherent surfaces cells tended to migrate (supplementary material Fig. S1). We performed FACS, qRT-PCR, immunophenotype analysis and cytogenetic analysis. (Fig. 1A) shows representative images of DPPSCs morphology at P5, P10 and P15. DPPSCs are small-sized cells with large nuclei and low cytoplasm content, without the typical flat and elongated MSC appearance. The morphology of DPPSCs cultured in a Cell Carrier 3D glass scaffold was also examined using scanning electronic microscopy (supplementary material Fig. S2). Immunofluorescence assays for SSEA4, OCT3/4 and NANOG showed that cells were positive for all three markers and that SSEA4 localised in the cytoplasm, whereas embryonic transcription factors were located in the nucleus (Fig. 1B).

The development of therapeutic strategies depends on the ability of stem cells to undergo large scale in vitro amplification, which can be associated with genetic instability. 85% of DPPSCs exhibited a normal karyotype with no presence of any aneuploidy, polyploidy or any chromosome structural abnormality in metaphases after more than 65 passages (Fig. 1C).

Using transmission electron microscopy (TEM), we evaluated the morphology and integrity of the cells (Fig. 1D). A notable feature of DPPSCs is that they possess large nuclei relative to cytoplasm volume, which is also a characteristic of ES cells.

Short-CGH analysis demonstrates genetic stability of DPPSCs as they showed the same genetic dose as a healthy control sample. A gain in X and a loss of Y chromosome dose can be seen, where this is due to sex differences: DPPSCs were extracted from a female patient, whereas the cells onto which the hybridisation was performed were from a male donor (Fig. 1E).

In order to further characterise the population, we analysed the cells by flow cytometry and found that the population was CD105$^+$, CD146$^+$, CD45$^-$, CD34$^-$, STRO1$^+$, TRA1-60$^-$, OCT3/4$^+$ and NANOG$^-$ (Fig. 2A,B). Double staining for OCT3/4 and NANOG was also carried out showing a 19.55% of double positive cells (Fig. 2C). Some differences in the expression level were found between different passages. Interestingly, percentage of SSEA4$^+$, OCT3/4$^+$ and NANOG$^+$ increased with passages in DPPSCs, whereas in DPMSCs, they remained negative (supplementary material Table S2). We also looked for cells expressing embryonic markers in pulp tissues from donors of different ages on the day of extraction (supplementary material Fig. S3). The percentage of SSEA4$^+$ cells increased with age, whereas the number of OCT3/4$^+$ and CD13$^+$ cells decreased with age. In addition, we found that embryonic markers were still expressed in DPPSCs from 58-year-old patients.

RNA was isolated from DPPSCs at P15, and expression of *OCT3/4*, *SOX2* and *TERT* was analysed by RT-PCR (Fig. 2D). Western blot analysis of OCT3/4 expression was performed in DPPSCs at P5, P10, P15 and P20. NTERA cells and bone marrow multipotent adult progenitor cells (BM-MAPCs) were used as positive controls, and Schwann cells and DPMSCs were used as negative controls (Fig. 2E). Expression of OCT3/4 in DPPSCs was maintained until at least P20.

The pluripotency of DPPSCs was assessed *in vivo* by teratoma formation. The injection of DPPSCs (P15) into nude mice resulted in the formation of teratoma-like structures that contained tissues derived from all three embryonic germ layers. DPPSCs from two different donors gave similar results. DPMSCs from the same donors were used as negative controls, and did not give rise to teratoma formation (Fig. 2F). We performed the teratoma assays with four groups with a total number of seven 8-week-old nude mice (Samtako Bio Korea, Seoul, Korea) were anesthetized with diethyl ether. Group 1:2 mice injected with cells from the 14-year-old donor. Group 2:2 mice injected with cells from the 17-year-old donor. Group 3:2 mice injected with cells from the 28-year-old donor. Group 4:1 mice injected with Matrigel (BD). Four out of seven mice injected developed teratoma-like forms with sizes of 0.6 to 1 cm just in the left side, where DPPSCs were injected (two mice from group 1, and two from group 3). In contrast, when DPMSCs from the same donor were injected, no teratoma formation was observed (Fig. 2E). All the mice from group 2 died at 8 or 12 days after injection. This result was unexpected and no obvious explanation occurred to us.

Staining with H&E showed the formation of multiple adult structures with origins in different embryonic layers (Fig. 2G; supplementary material Fig. S4) such as chondroid tissue, chondroid matrix, fibroblasts and collagen fibres, adipose tissue and endothelium (Fig. 2L), gut-like epithelium (Fig. 2M), and neural-like tissue such as nerve and keratin (Fig. 2N).

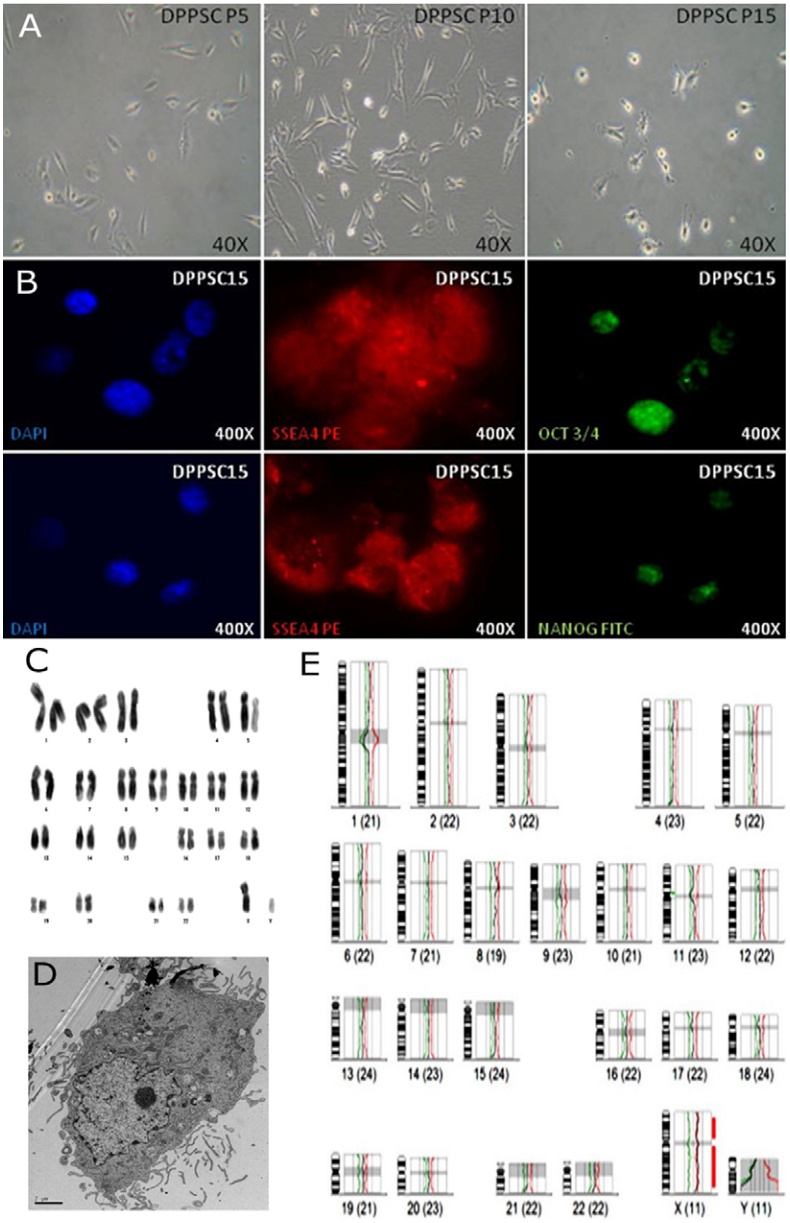

Fig. 1. Characterisation and cellular morphology of pluripotent stem cells obtained from dental pulp (DPPSCs) by in vitro expansion. (**A**) Morphology of DPPSCs at different passages (P5, P10 and P15). (**B**) Analysis of DPPSC immunophenotype by confocal microscopy shows the expression of SSEA4 PE (28±1.13%) together with OCT3/4 FITC (60.3±5.3%) or NANOG FITC (21.3%±3.6). Average of three independent experiments. (**C**) Cytogenetic analysis of undifferentiated DPPSCs (P15) show 46 XY without aneuploidy or polyploidy; chromosome structural abnormalities were not detected. (**D**) Cells examined by transmission electron microscopy show large nuclei and small cytoplasmic volume. Scale bar: 10 µm. (**E**) Short-CGH analysis showing genetic stability of DPPSCs from a female donor (n=3).

Immunohistochemical staining was performed to evaluate the expression of embryonic markers after 3 weeks (Fig. 2H–K). Although DPPSCs expressed embryonic markers when they were undifferentiated, expression of these genes was lost during differentiation, and very few cells were positive for embryonic markers at 3 weeks. Antihuman antibodies were used to confirm that the tissues formed were of human origin.

The ability of DPPSCs to form EBs was studied using a micropatterned culture surface and centrifugal force (Fig. 3A). After 5 days of culture, the morphology of EBs was evaluated by light microscopy (Fig. 3B). EBs exhibited the typical spherical and well-limited appearance of EBs formed from ES cells. Alkaline phosphatase (ALP) staining was performed to confirm the stem-like properties of the EBs (Fig. 3C). Furthermore, the EBs continued to express embryonic markers such as OCT3/4 and NANOG at day 5, as observed by immunofluorescence (Fig. 3D,E). The expression of embryonic markers and lineage specific markers was studied by RT-PCR. The results showed that DPPSCs and EBs from DPPSCs expressed embryonic markers such as OCT3/4, NANOG and SOX2 as well as other lineage markers as SOX1, BDNF, MIXL1, GATA4 and GATA6 with levels comparable to iPS cells. DPMSCs did not express these markers (Fig. 3F). To confirm the results, a qRT-PCR was performed to check the expression of the same genes, using iPS cells as a positive control. Levels of OCT3/4 and NANOG were higher in DPPSCs than in EBs whereas lineage markers as GATA 4, GATA6 and MIXL1 were higher in EBs (Fig. 3G).

The protein expression profile of DPMSCs (Fig. 4A) was substantially different from that of DPPSCs. Specifically, levels of embryonic markers (OCT3/4, NANOG and SSEA4) were very low, whereas levels of CD73 and STRO1 were high in DPMSCs. Comparative FACS analysis was carried out on different passages of populations from both cell types isolated from 14-, 17-, 18-, 28- and 38-year-old donors (supplementary material

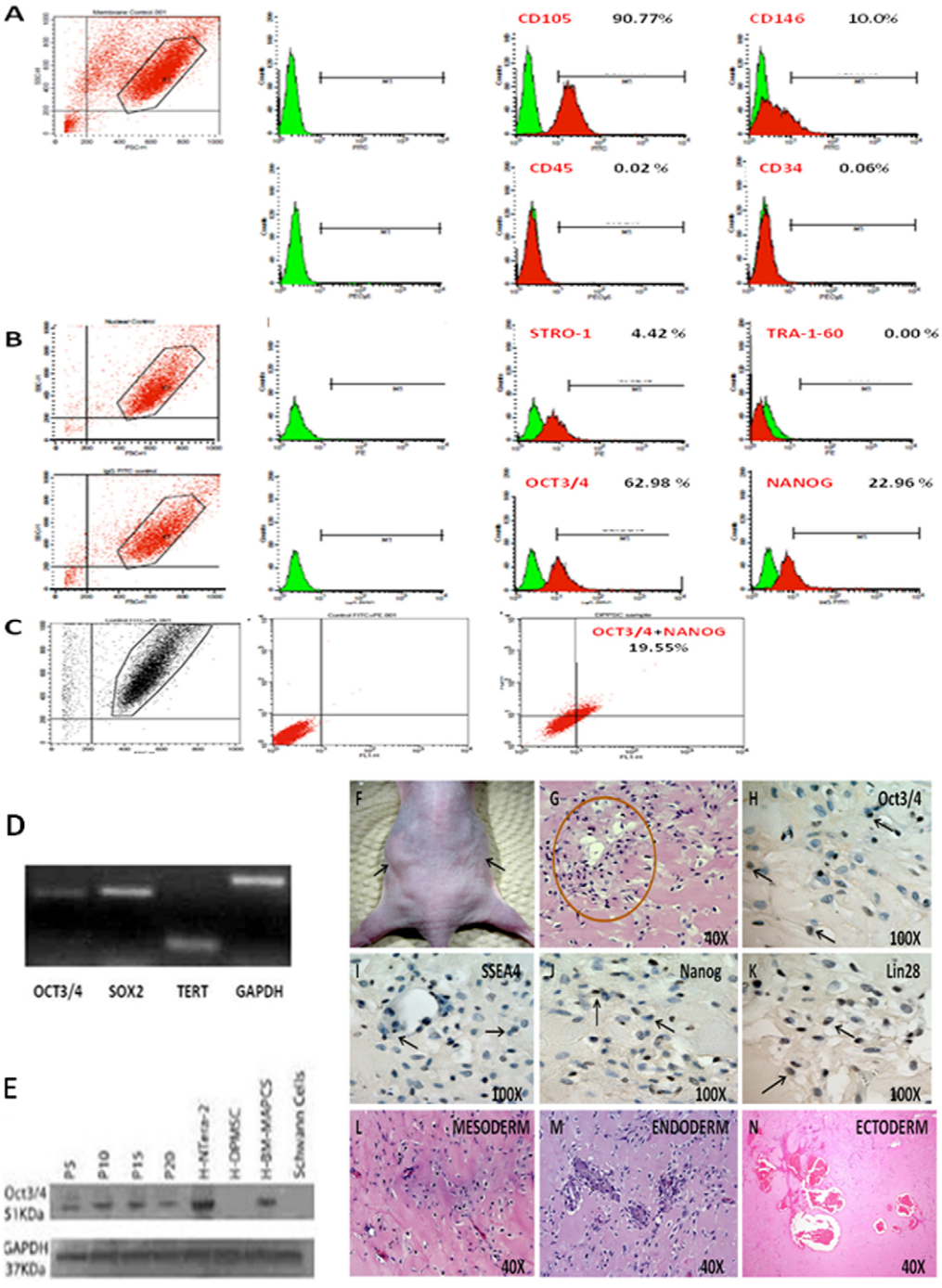

Fig. 2. FACS characterisation, gene expression of P15 DPPSCs and teratoma formation. (**A**) FACS analysis of P15 DPPSCs for membrane markers: CD105 (90.77±2.28%), CD146 (13.17±0.68%), CD45 (0.02±0.39%) and CD34 (0.06±0.05); (**B**) FACS analysis of P15 DPPSCs for nuclear markers: STRO1 (4.42±1.23), TRA1 (0.00±0%), OCT3/4 (62.98±5.22%) and NANOG (22.96±2.58%). (**C**) Analysis by FACS of DPPSCs with double staining (19.55%) for OCT3/4 FITC (27.08%) and NANOG PE (25.94±2.51). Expressed as average of three independent experiments. (**D**) RT-PCR of *OCT3/4*, *SOX2*, *TERT* and *GAPDH* of DPPSC P15 in 2D culture. (**E**) OCT3/4 detection by western blot of DPPSCs at different passages compared with DPMSCs. NTERA cells and BM-MAPCs were used as positive controls, and Schwann cells and DPMSCs were used as negative controls. (**F**) Transplantation of P15 DPPSCs and DPMSCs isolated from the same donor from different ages (14, 17, 28 years old) into immunodeficient mice resulted in apparent teratoma-like formation (left flank) after 5 weeks; DPMSCs P15 were used as a negative control (right flank). H&E staining of teratoma-like structures induced by DPPSCs show the presence of tissues from mesoderm, endoderm and ectoderm. (**G**) H&E staining of teratoma-like structure after 3 weeks. Circle highlights zone that is magnified in H–K. (**H**) Immunohistochemical staining for OCT3/4. (**I**) Immunohistochemical staining for SSEA4. (**J**) Immunohistochemical staining for NANOG. (**K**) Immunohistochemical staining for LIN28. Immunohistochemical staining shows embryonic markers SSEA4, LIN28, OCT3/4 and NANOG (black arrows). (**L**) H&E staining showing chondroid tissue, chondroid matrix, fibroblasts and collagen fibres. (**M**) H&E staining showing gut-like epithelium. (**N**) H&E staining showing nerve-like tissue and keratin.

Table S2). The two cell types were easily distinguishable by their morphology. DPMSCs showed the typical flat and elongated appearance of mesenchymal cells, whereas DPPSCs were smaller and more spherical in shape (Fig. 4B). Cell diameters ranged from 8–12 μm for DPPSCs and 12–19 μm for DPMSCs (Fig. 4C).

Multiscreen-MIC plate carbonate filters were used to evaluate the migratory capacity of DPPSCs. Although they came from the same donor and were from the same passage, more DPPSCs migrated across the filters than DPMSCs (Fig. 4D). To compare the adhesive ability of DPPSCs and DPMSCs, the expression of integrin CD29 was evaluated by FACS analysis. The results showed that 99.6% of DPPSCs expressed integrin CD29, compared to only 82.3% of DPMSCs (Fig. 4E).

Although they were the main population, DPPSCs coexisted in culture with other cell types, such as mesenchymal stem cells from the dental pulp (DPMSCs), due to the lack of a stringent selection when performing primary culture and successive cultures with DPPSC medium. The two populations were indistinguishable from each other by FACS analysis, although size was known to be different. The percentages of OCT3/4, NANOG and CD73 in different gates depending on size and complexity were insufficient to distinguish the two populations as well (Fig. 4F,G; supplementary material Table S3).

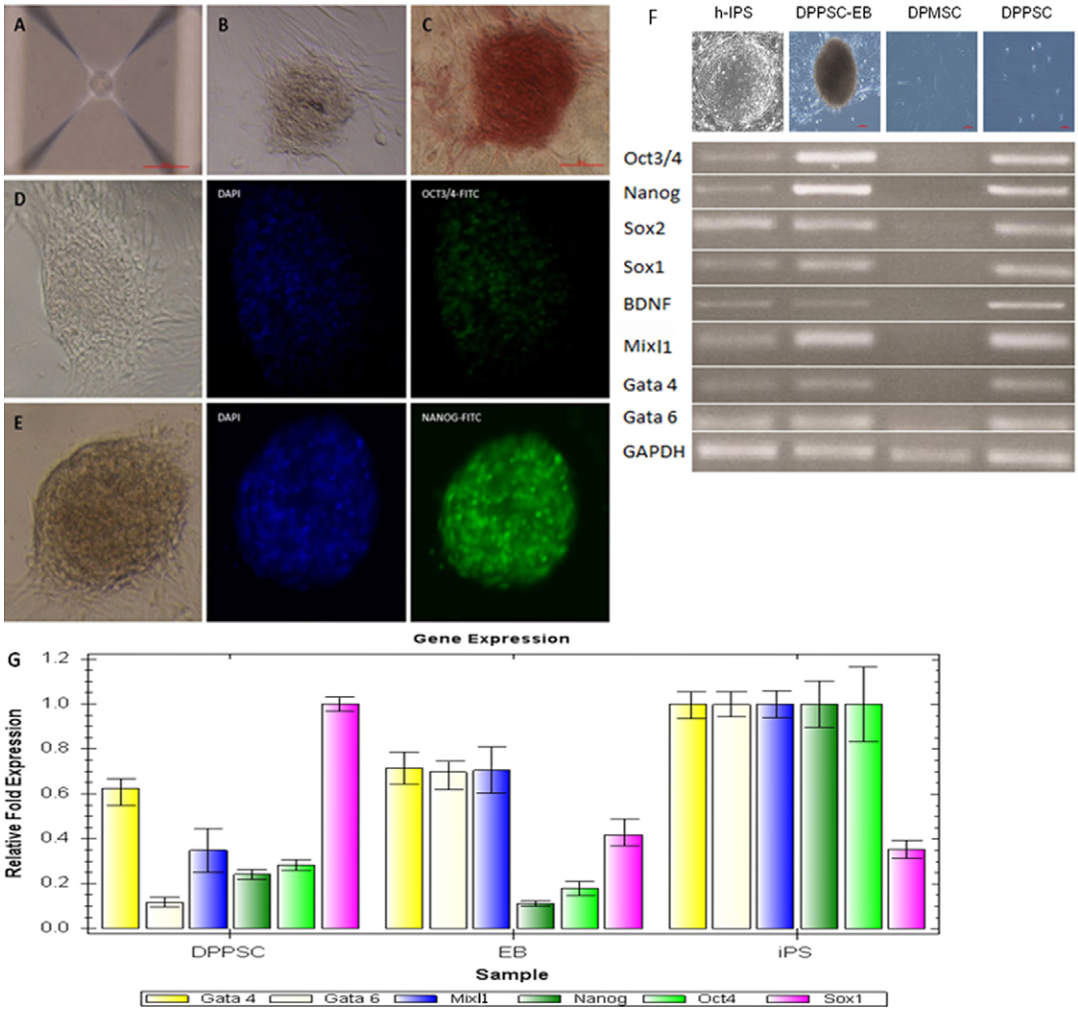

Fig. 3. Generation of DPPSC P15 embryoid bodies. (**A**) AggreWell system (Stem Cell Technologies), which utilises a micropatterned culture surface and centrifugal forced aggregation to direct the formation of EBs by DPPSCs for 5 days. Scale bar: 100 µm. (**B**) Morphology of DPPSC embryoid bodies examined by light microscope. (**C**) Alkaline phosphatase staining of DPPSC embryoid bodies. Scale bar: 100 µm. (**D**) Immuno-phenotype analysis by fluorescence microscopy shows the expression of OCT3/4 FITC. (**E**) Immunostaining of DPPSC EBs generated by AggreWell system with NANOG FITC. (**F**) RT-PCR analysis of *OCT3/4*, *NANOG*, *SOX2*, *SOX1*, *BDNF*, *MIXL1*, *GATA4*, *GATA6* and *GAPDH*, comparing expression of hIPSCs, EBs from P15 DPPSCs and P15 DPMSCs and DPPSCs. (**G**) qRT-PCR analysis of *GATA4*, *GATA6*, *MIXL1*, *NANOG*, *OCT3/4*, *SOX1* in DPPSCs P15, EBs from DPPSCs and hiPSC. Expression levels were normalized to GAPDH. Data represented as means ± s.d. of three independent experiments.

To further characterise the two cell populations, we performed magnetic separation using a human PE selection kit. Cells positive for CD73 were stained with a PE-conjugated antibody, and we extracted RNA from both the $CD73^{-}$ and $CD73^{+}$ populations after separation. RT-PCR was performed to determine embryonic gene expression. The $CD73^{-}$ population expressed *TERT*, *OCT3/4* and *SOX2*, but the $CD73^{+}$ cells did not (Fig. 4H). This confirmed our previous assumption that DPPSCs coexisted with DPMSCs when cultured in vitro.

We also observed a correlation between the embryonic development stages of the third molar and the percentage of OCT3/4 and NANOG expression by FACS analysis in pulp tissues from donors of different nolla stages (6–10) and different ages on the same day of extraction ($n=14$ samples) (supplementary material Table S4). To determine the relationship between specific DPPSCs markers and tooth nolla stages, the expression profiles were subjected to regression analysis using nolla stage as the independent variable to determine the subpopulation of DPPSCs. All the samples showed the presence of DPPSCs and low expression of the markers *OCT3/4* and *NANOG*.

To see whether the culture conditions were a key aspect for the maintenance of the different phenotypes between DPPSCs and DPMSCs, we cultured each type of cell with the medium of the other one. After one week changing the medium every 2 or 3 days we observed some phenotypic changes (Fig. 5A). DPPSCs acquired a longer and flattered shape whereas some of the DPMSCs became smaller and with a morphology resembling DPPSCs. Changes were easier to see in DPPSCs culture in mesenchymal media than in the other way. We checked the expression of the embryonic markers that differ between the two cell types. We observed that DPPSCs cultured in mesenchymal medium lost the expression of *NANOG*, whereas the *OCT3/4* levels only decreased. In the case of DPMSCs cultured in DPPSC

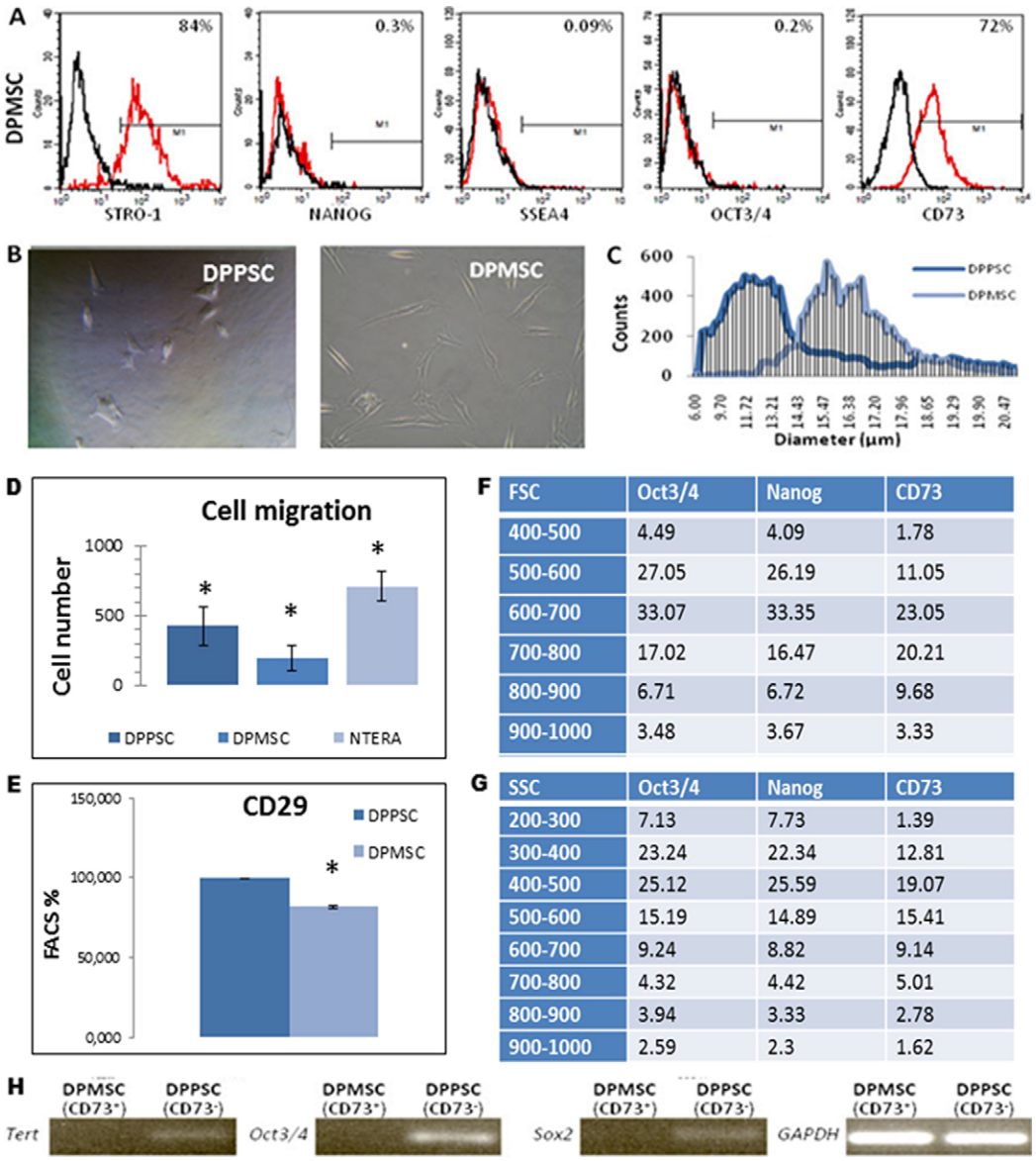

F

FSC	Oct3/4	Nanog	CD73
400-500	4.49	4.09	1.78
500-600	27.05	26.19	11.05
600-700	33.07	33.35	23.05
700-800	17.02	16.47	20.21
800-900	6.71	6.72	9.68
900-1000	3.48	3.67	3.33

G

SSC	Oct3/4	Nanog	CD73
200-300	7.13	7.73	1.39
300-400	23.24	22.34	12.81
400-500	25.12	25.59	19.07
500-600	15.19	14.89	15.41
600-700	9.24	8.82	9.14
700-800	4.32	4.42	5.01
800-900	3.94	3.33	2.78
900-1000	2.59	2.3	1.62

Fig. 4. Comparison of morphology and protein profiles in DPPSCs and DPMSCs. (**A**) Immuno-phenotype by FACS analysis of P15 DPMSCs isolated from dental pulp. Expression of STRO-1 (84.12±1.67%), NANOG (0.28±0.33%), SSEA4 (0.09±0.12%), OCT3/4 (0.2±0.2%), CD73 (72±2.69%) is shown as the average of three independent experiments. (**B**) Comparison of morphology of DPPSCs and DPMSCs from the same donor and the same passage (P15). (**C**) Cell diameters of DPPSCs and DPMSCs measured by Scepter Millipore. (**D**) Cell migration capacity of P15 DPPSCs and DPMSCs from the same donor and hNTERA cells, which were used as a positive control, was determined using a Multiscreen-MIC Plate polycarbonate filter (8 µm pore size), incubated at 37°C, 5% CO_2 for 6 hours. Significance was set at $*P \leq 0.05$ ($n=5$). (**E**) Analysis by FACS for CD29 expression in a 3D culture of DPPSCs at P15 (99.6±0.61%) and DPMSCs at P15 (82.3±7.88%). (**F**,**G**) Analysis of the different populations coexisting in DPPSC cell culture in terms of their cell size (FSC) and their complexity (SSC). Percentage of $OCT3/4^+$, $NANOG^+$ or $CD73^+$ cells in every gate analysed is shown with respect to the total. (**H**) RT-PCR for embryonic genes *TERT*, *OCT3/4* and *SOX2* of the two separated cell populations of DPPSC ($CD73^-$) and DPMSC ($CD73^+$) cultures.

medium, cells gained the expression of both *OCT3/4* and *NANOG* (Fig. 5B).

To confirm the pluripotent capacity of DPPSCs we performed three in vitro differentiation assays in which DPPSCs were induced to give rise tissues from all three germ layers.

Mesoderm differentiation

We analysed the ability of DPPSCs to differentiate into osteoblasts in 2D by immunofluorescence and qRT-PCR. The morphology of DPPSCs cultured with osteogenic media changed over three weeks of differentiation, resulting in cells with a bone-like appearance (Fig. 6A) that expressed the osteoblast marker OSTEOCALCIN (Fig. 6B). The differentiated cells showed upregulated expression of specific bone tissue genes, such as *ALP*, *OSTEONECTIN*, *OSTECALCIN* (Fig. 6C), *OSTEOPONTIN*, *COLLAGEN I*, *COLLAGEN III* and *BMP2*, whereas *NANOG* was downregulated (supplementary material Table S5). Human bone cDNAs were used to normalise the data, *GAPDH* was used as a housekeeping gene and DPPSC undifferentiated dental pulp cells were used as a negative control (data not shown). *ALP*, *OSTEONECTIN* and

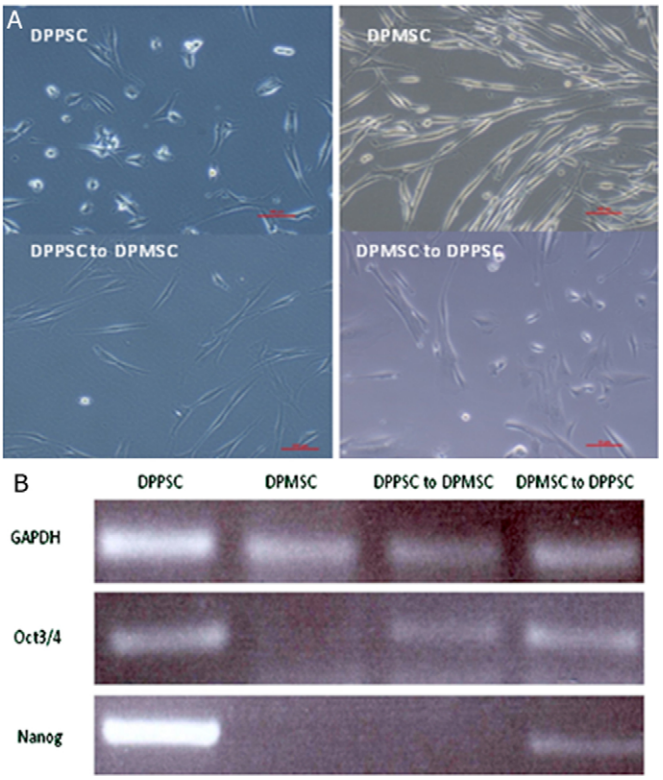

Fig. 5. Changes in expression of embryonic markers upon changing the culture conditions. (**A**) Changes in morphology in DPPSCs and DPMSCs when they were cultured in the medium of the other cell type for 1 week. (**B**) Changes in expression of embryonic markers in P10 DPPSCs and DPMSCs when cultured in the medium of the other cell type for 1 week (2 passages). Expression of *OCT3/4* and *NANOG* was analysed by RT-PCR.

OSTEOCALCIN expression increased in the first, second and third weeks of differentiation. We also observed a decrease in *NANOG* expression. To confirm bone-like cell differentiation, we used Alizarin Red to stain extracellular matrix deposits consisting of hydroxyapatite, calcium and magnesium salts (Fig. 6D). Taken together, these assays demonstrate that DPPSCs could efficiently differentiate into bone-like tissue and express specific bone tissue genes.

Differentiation was also performed using a Cell Carrier 3D glass scaffold. When cultured in osteogenic differentiation medium, DPPSCs derived into bone-like tissue that was able to synthesise typical bone structures, such as collagen and cortical structures that were detectable by SEM analysis (Fig. 6E; supplementary material Fig. S5). The 3D differentiation was also confirmed by qRT-PCR. During three weeks of differentiation, *ALP*, *COLLAGEN I* and *COLLAGEN III* expression steadily increased, whereas the embryonic markers *NANOG* and *OCT3/4* decreased each week (Fig. 6F). Functional activity was determined by quantifying ALP activity (Fig. 6G) and the calcium secretion (Fig. 6H) every week for three weeks. Both ALP activity and the calcium secretion increased significantly on days 7, 14 and 21 of osteogenic differentiation.

To demonstrate the capacity of DPPSC to differentiate into other tissues of the mesoderm cap, we performed a vessel-derived endothelial cell differentiation, in which DPPSCs were cultured with basal media (2% FBS, 50 ng/ml VEGF, 10 ng/ml bFGF) for

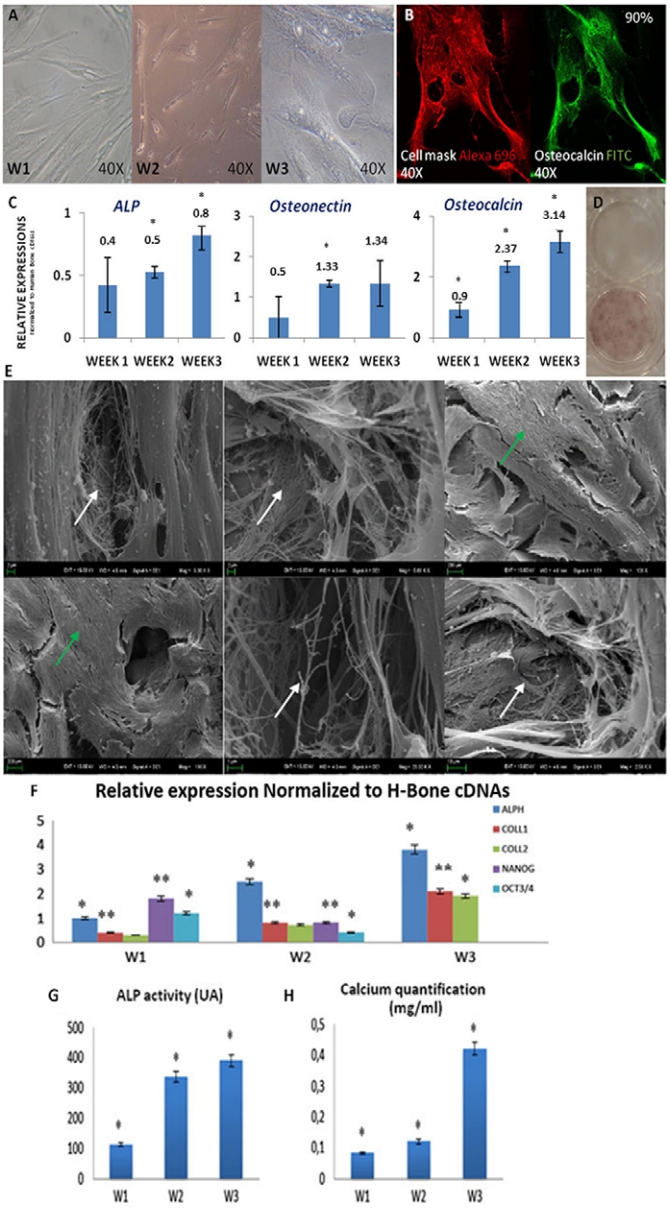

Fig. 6. Differentiation of P15 DPPSCs into mesoderm. (**A**) Cell morphology during osteogenic 2D differentiation at weeks 1, 2 and 3 (W1, W2 and W3). (**B**) Immunofluorescence shows the expression of osteocalcin FITC in the cytoplasm and cell mask Alexa Fluor W696. (**C**) *ALP*, *OSTEONECTIN* and *OSTEOCALCIN* detection by qRT-PCR at different time points during 2D osteogenic differentiation of DPPSCs ($n=3$, from 14-, 17- and 28-year-old donors, $^*P<0.05$). The mRNA levels were normalised to *GAPDH* (a housekeeping gene). The relative expression was normalised to human cDNAs, which is normalised to 1. (**D**) Alizarin Red staining of DPPSCs after 3 weeks of 2D osteogenic differentiation. (**E**) Scanning electron microscopy image of 3D differentiation of DPPSCs at P15 using a Cell Carrier 3D glass scaffold for 21 days into mesoderm tissues. Bone-like tissue, collagen (white arrow) and cortical (green arrow) structures were observed. (**F**) Analysis of the expression of *ALP*, *COLLAGEN I*, *COLLAGEN II*, *NANOG* and *OCT3/4* by qRT-PCR during 3 weeks of 3D differentiation. The mRNA levels were normalised to *GAPDH*. The relative expression was normalised to human cDNA from bone ($n=3$, from 14-, 17- and 28-year-old donors, $^*P<0.05$, $^{**}P\leq0.001$), which was designated as 1. (**G**) ALP activity at different time points of osteogenic differentiation in 3D for 21 days. Data are presented as means ± s.d. ($n=3$). $^*P\leq0.05$. (**H**) Calcium quantification at different time points of osteogenic 3D differentiation for 21 days. Data are presented as means ± s.d. ($n=3$). $^*P\leq0.05$.

three week. We observed an increase in the expression of specific endothelial genes, such as *FLK1* and *CD14* (by qRT-PCR) and FLK1 (by immunofluorescence) (supplementary material Fig. S6).

Endoderm differentiation

Another differentiation assay was performed to induce DPPSCs to generate cells from the endodermal lineage, specifically hepatocyte-like cells. DPPSCs cultured in 2D with hepatogenic media for the three weeks showed altered morphologies, with some cells adopting a polygonal shape similar to hepatocytes (Fig. 7A). Expression of the typical hepatic protein albumin (ALB) was detected by immunofluorescence (Fig. 7B). Using qRT-PCR, we demonstrated that differentiated cells expressed the hepatic nuclear factors *HNF3β*, *HNF6* and *GATA4* (Fig. 7C). The expression levels of *α-fetoprotein* (*AFP*), *ALB*, *CEBPA* and *NANOG* were also determined (supplementary material Table S6). We also observed a decrease in *NANOG* during the 3 weeks of differentiation (data not shown). Human liver cDNAs (Ambion) were used to normalise the data and *GAPDH* was used as the housekeeping control (data not shown). The levels of secreted ALB increased significantly over three weeks of differentiation (Fig. 7D). These results indicate DPPSCs can upregulate endoderm markers and differentiate into hepatic-like cells, both genetically and functionally, upon hepatogenic induction.

Cell Carrier 3D glass scaffolds were also used to perform the endoderm differentiation. After 21 days of 3D culture with hepatogenic media, some hepatic structures were seen by SEM analysis, including large and small pores with a fenestra-like appearance, the surfaces of sinusoidal endothelial cells and ultra-structures of sinusoidal endothelial cells (Fig. 7E; supplementary material Fig. S7). qRT-PCR was performed to evaluate the expression of hepatic specific genes *ALB*, *AFP* and *CYP3A4*. Expression of these markers increased each week, whereas the embryonic markers *NANOG* and *OCT3/4* expression decreased (Fig. 7F). Functional activity was determined by quantifying

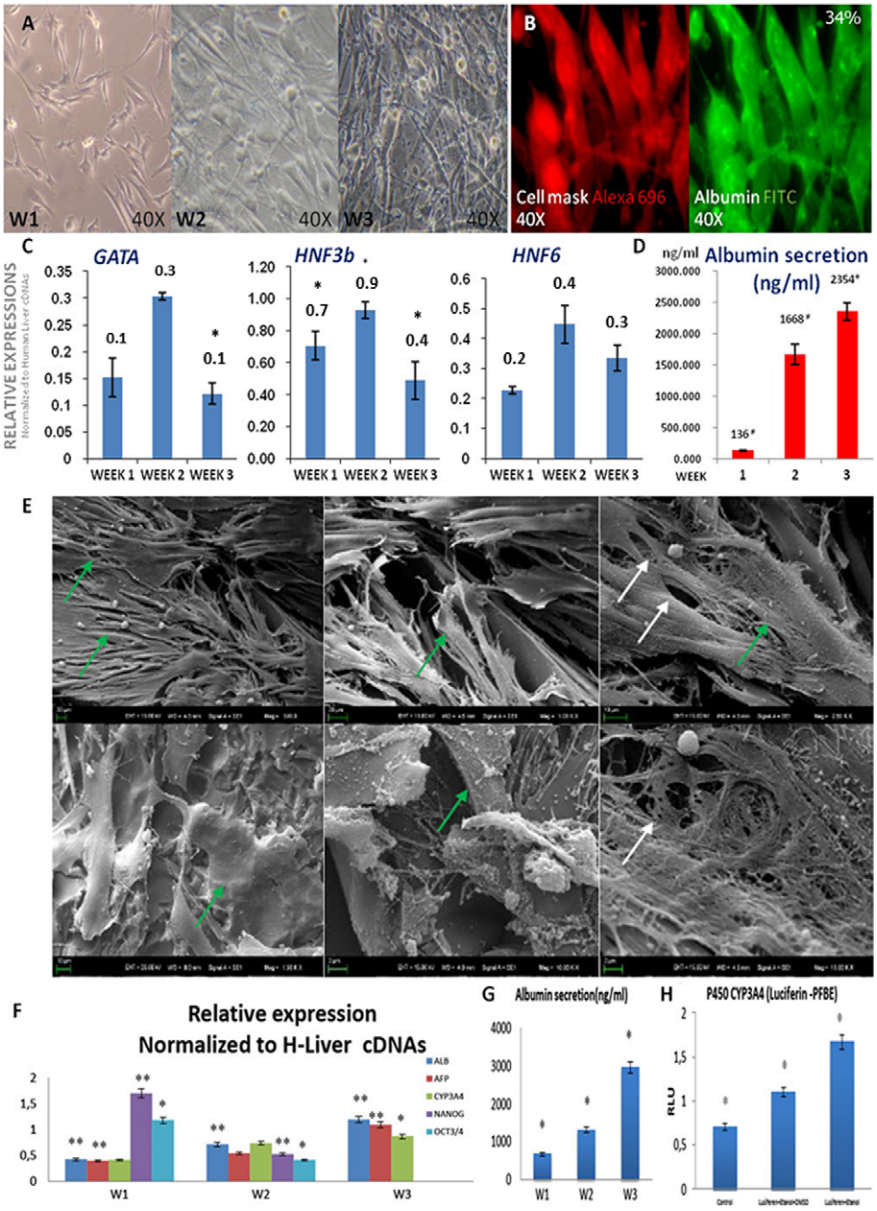

Fig. 7. Differentiation of P15 DPPSCs into endoderm. (**A**) Cell morphology of DPPSCs at different time points (weeks 1, 2 and 3) during 2D hepatic differentiation. (**B**) Immunofluorescence at day 21 of 2D differentiation into hepatocyte-like cells shows the expression of ALB FITC in the cytoplasm and cell mask Alexa Fluor W696. (**C**) qRT-PCR detection of *GATA4*, *HNF3β* and *HNF6* in 2D differentiated DPPSCs ($n=3$, $^*P<0.05$). The mRNA levels were normalised to *GAPDH*. The relative expression was normalised to human cDNAs from liver cells, assigned as 1. (**D**) ALB synthesis analysis at different days of 2D differentiation into hepatocyte-like cells. Data are presented as mean ± s.d. ($n=3$ from 14-, 17- and 28-year-old donors). $^*P\leq0.05$. (**E**) Scanning electron microscope image of 3D endoderm differentiation of DPPSCs at P15 after 21 days on a Cell Carrier 3D glass scaffold. Hepatic-like cells with large and small open pores are observed that have a fenestrated appearance (white arrow). The ultrastructure of sinusoidal endothelial cells (green arrow) and the surface of sinusoidal endothelial cells can also be observed. (**F**) qRT-PCR detection of *ALB*, *AFP*, *CYP3A4*, *NANOG* and *OCT3/4* in DPPSCs differentiated into a 3D hepatic lineage ($n=3$, $^*P<0.05$, $^{**}P\leq0.001$). The mRNA levels were normalised to *GAPDH*. The relative expression was normalised to human cDNAs from liver cells, which were assigned as 1. (**G**) ALB synthesis analysis at different days of 3D differentiation into hepatocyte-like cells. Data are presented as means ± s.d. ($n=3$). $^*P\leq0.05$. (**H**) Cytochrome P450-3A4 Metabolic Activity Assay. Data are presented as means ± s.d. ($n=3$). $^*P\leq0.05$.

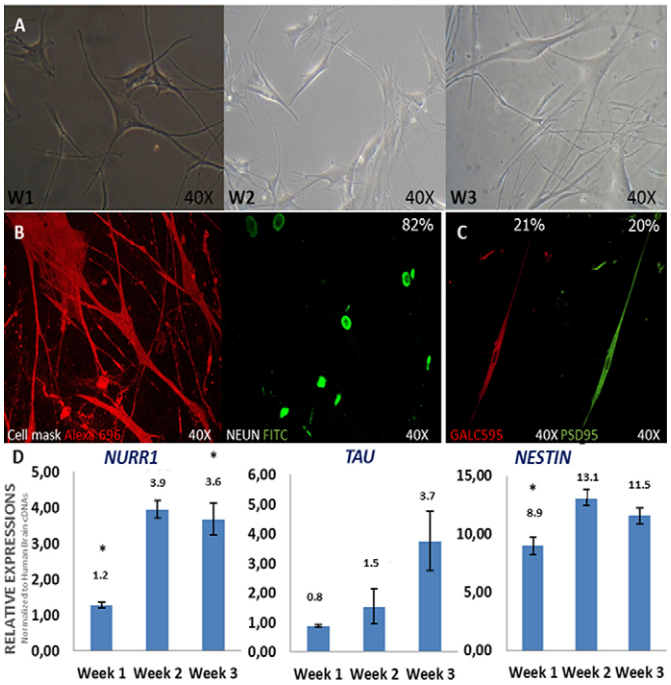

Fig. 8. Neuroectoderm differentiation of P15 DPPSCs. (**A**) Image by optical microscopy of the morphology of cells differentiated into neural-like cells at different time points (weeks 1, 2 and 3). (**B**) DPPSCs differentiated into neural-like cells after 3 weeks showed expression of NEUN FITC and cell mask Alexa Fluor W696. (**C**) DPPSCs differentiated to neural-like cells after 3 weeks showed expression of GALC595 and PSD95. (**D**) Analysis of the expression of *NURR 1, TAU* and *NESTIN* by qRT-PCR during the three weeks of differentiation. mRNA levels were normalised to *GAPDH*. The relative expression was normalised to human cDNA from brain cells ($n=3$, from 14,- 17- and 28-year-old donors, $^*P<0.05$), which was designated as 1.

ALB secretion (Fig. 7G) and P450 CYP3A4 activity (luciferin-PFBE) (Fig. 7H). As in 2D differentiation cultures, the levels of secreted ALB increased over time. The activity of CYP3A4 in differentiated cells was higher than in undifferentiated control cells. Both experiments were performed in triplicate.

Ectoderm differentiation

Finally, DPPSCs were able to follow a neuroectodermal differentiation pathway in 2D cultures. The morphology of differentiated cells was phenotypically clearly similar to neuronal cells (Fig. 8A). Immunofluorescence staining showed that differentiated DPPSCs expressed neuronal tissue-specific proteins such as NEUN (Fig. 8B), GALC 595 and PSD95 (Fig. 8C). qRT-PCR analysis showed that expression levels of *TAU* increased with time, and that the levels of *NURR1* and *NESTIN* increased during weeks one and two and then plateaued at week three (Fig. 8D). *GFAP*, *MBP* and *SOX1* also increased during the first, second and third weeks, whereas *NANOG* expression decreased during differentiation (supplementary material Table S7). Human brain cDNA (Ambion) was used to normalise the data and GAPDH was used as the housekeeping control (data not shown).

Discussion

Several populations of stem cells have been isolated from different parts of the human tooth and all of them have been shown to have generic mesenchymal stem cell-like properties (Laino et al., 2005). These cells express markers associated with the endothelium and/or the smooth muscle, such as Stromal-derived factor 1 (*STRO1*), Vascular cell adhesion molecule 1 (*VCAM1*), Melanoma-associated antigen MUC18 (*MUC18*) and smooth muscle actin (Téclès et al., 2005). Other reports have described the presence of a lateral population of stem cells in the dental pulp (Casagrande et al., 2006; Liu et al., 2006; Rizzino, 2009; Sloan and Smith, 2007; Volponi et al., 2010; Zhang et al., 2006b). However, there has been no previously published reference to the presence of a population of cells in dental pulp with the protein profile $SSEA4^+$, $OCT3/4^+$, $NANOG^+$, $Nestin^+$, $SOX2^+$, $LIN28^+$, $CD13^+$, $CD105^+$, $CD34^-$, $CD45^-$, $CD90^{low}$, $CD29^+$, $CD73^{low}$, $STRO1^{low}$ and $CD146^-$ (Oda et al., 2010), as presented in this work. OCT3/4, NANOG and SOX2 are indispensable for indefinite stem cell division, without affecting differentiation potential or the capacity for self-renewal. The functional importance of *SOX2* and *NANOG* genes in altering the progenitor status has also been clearly demonstrated (Hanna et al., 2010; Ratajczak et al., 2008; Takahashi and Yamanaka, 2006; Yu et al., 2007; Zuba-Surma et al., 2009). *NANOG* has been reported to be a key gene for maintaining pluripotency, as shown by the capacity for multilineage differentiation and perpetual self-renewal of cells expressing this gene. Although DPPSCs share some features with other populations of stem cells in the tooth, they differ in other aspects, such as gene expression and differentiation potential (Hirata et al., 2010) due to their embryonic-like properties. In this work, we observed the formation of EB-like structures with characteristics similar to embryonic stem cells and MAPCs (Braccini et al., 2005; Verfaillie, 2005).

Both DPMSCs and DPPSCs are obtained from dental pulp using the same isolation protocol. Distinction of these different cell populations is dependent on the density at which the cells are seeded and the culture medium. The use of media that contain growth factors EGF, PDGF and LIF, allows maintenance of the pluripotent state of DPPSCs. There has been no other report of the use of a similar medium to culture stem cells from the dental pulp, so it seems likely that this media formulation is key for maintaining DPPSCs with typical stem cell properties. In culture, however, DPPSCs display heterogeneity that can be explained as a consequence of their spontaneous differentiation and the lack of clonality upon their isolation. As previously shown, other stem cell cultures undergo the same processes; for example, MAPC cultures are heterogeneous, and two cell populations with different phenotypes (large and small) coexist in the same culture (Verfaillie, 2005). Here, we have demonstrated that the DPPSC population coexists in culture with other cell types, such as DPMSCs, and that the populations were different from one another, as they differed in pluripotency gene expression after magnetic separation by CD73. It seems plausible that both cell types have a common progenitor, but the relationship between them is still unclear. The fact that DPPSCs express some embryonic markers but the other population does not suggests that these populations may be at a different level of the differentiation hierarchy, and that DPPSCs may be the progenitors that gave rise to the other populations. Further experiments will be needed in order to test this hypothesis.

The third molars are the most common source of dental stem cells, because wisdom tooth extraction is widely performed and the teeth are usually considered to be medical waste (Otaki et al., 2007; Yang et al., 2007). Because the third molar is the last tooth

to develop in humans, it is normally in an early stage of development and is capable of yielding an optimum quantity of dental pulp tissue for the isolation of DPSCs (Gandia et al., 2008; Laino et al., 2006; Leeb et al., 2010; Morsczeck et al., 2009; Smith et al., 2009; Atari et al., 2011; Zhang et al., 2006a). Although the percentage of DPPSCs decreases with age, a population of these cells was always present, even in older patients. Multipotent cells that have a certain degree of pluripotency, because they are derived from early embryonic cells and maintained in the adult stage (Ebert et al., 2009), have been found in adult tissues, such as very small embryonic-like (VSEL) stem cells in the bone marrow. These studies, together with the data shown here, indicate that the dental pulp could be an important source of cells with pluripotent characteristics. We speculate that DPPSCs could be derived from residual undifferentiated cells in the dental pulp. However, this hypothesis requires further testing. The characteristics unique to these cells are still under investigation, but the current evidence opens to the way for future comparative studies of the regenerative potency of DPPSCs and stem cells from other sources. In addition, the possibility of freezing these cells following molar extraction seems feasible, as is currently performed with cells obtained from the umbilical cord.

In this paper, we have shown that DPPSCs have pluripotent-like properties that have not been found in cells of any other adult source to date. The ability to form EB-like or teratoma-like structures has been thought to be exclusive to ES or iPS cells (Benton et al., 2009; Maltman and Przyborski, 2010). With this finding, a new field of investigation can be opened. If one population of cells found in adult individuals can achieve true pluripotency, there may be other populations with the same or similar properties that have yet to be discovered. The relationship between DPPSCs and iPS cells should also be investigated. The induction of iPS cells seems to be easier from stem cells than from differentiated cells (Illich et al., 2011). It could be that a reprogramming process occurs in DPPSCs, but not in differentiated dermal fibroblasts. Thus, only DPPSCs could selectively expand when cultured in DPPSC media, but other cells from the dental pulp could not undergo the reprogramming process needed to acquire pluripotency. Importantly, the number of reprogramming factors needed for induced pluripotency could be reduced when using DPPSCs. Further studies are needed to answer these questions.

For therapeutic purposes, the reliability and safety of putative clinical applications for DPPSCs must be considered, especially the issue of genetic stability. We have demonstrated that DPPSCs show no chromosome abnormalities when cultured in vitro, such that we propose that DPPSCs are safe to use for clinical therapies. We propose that short-CGH should be used in stem cell research to determine genetic stability when cells are cultured in vitro, because s-CGH allows the detection of genetic abnormalities that could remain hidden with the current protocols, such as karyotype or FISH techniques. In addition, stem cells for therapeutic applications must be able to differentiate into different tissues. As we have shown, DPPSCs are capable of giving rise to mesodermal, endodermal and ectodermal tissues that express markers typical of osteoblasts (Atari et al., 2012), hepatocytes and neurons, respectively, as shown by qRT-PCR assays, in which all data were normalised to human cDNAs of the respective tissues. The use of 3D culture systems to carry out differentiation protocols represents an improved system that simulates the physiological in vivo environment (Dhawan et al., 2010; Undale et al., 2009). Based on images obtained by inverted optical microscopy (2D differentiation) and the pictures taken by SEM (3D differentiation), we observed tissue-specific structures, such as collagen fibres and fenestra-like structures, in 3D that were not seen in 2D.

These cells have properties that are not observed in other cells obtained from adult tissues, which could open a new range of possibilities for regenerative medicine. The results presented here suggest that DPPSCs may be useful for treating various disorders, such as those related to the loss of bone or some of the proteins synthesised related with the malfunction of liver cells. Further investigations are needed to fully characterise these cells.

Materials and Methods

Patient selection

Healthy human third molars extracted for orthodontic and prophylactic reasons were selected from 20 different patients of different sexes and ages (14–60 years old). The extraction procedure was kept simple to prevent tooth damage. Dental pulp tissues used for these experiments were obtained with informed consent from donors. All experiments were performed in accordance with the guidelines on human stem cell research issued by the Committee on Bioethics of the International University of Catalonia.

Primary cells obtained from human molar samples

Immediately after extraction, the third molars were washed using gauze soaked in 70% ethanol, followed by a wash with sterile distilled water. Holding the tooth with upper incisor forceps, an incision was made between the enamel and the cement using a cylindrical turbine bur. A fracture was made on the same line, and fragments of the tooth were placed in a Falcon flask containing sterile 1× PBS. The samples were rapidly transported to the laboratory and placed in Petri dishes in a laminar flow hood. Tissues were isolated from the dental pulp using a sterile nerve-puller file 15 and forceps. Cellular separation was completed by digesting the divided pulp tissue with collagenase type I (3 mg/ml) (Sigma) for 60 minutes at 37℃. Cells were then separated using an insulin syringe and centrifuged for 10 minutes at 275 ***g*** (RCF). The cell fraction was washed twice with sterile 1× PBS and centrifuged again for 10 minutes at 275 ***g*** at room temperature. Once collected, the cells were counted and seeded in DPPSC medium. In order to establish the primary culture, the cells were grown in 96-, 24- and 6-well culture dishes and in 150 ml flasks coated with 100 ng/ml human fibronectin inside a 5% CO_2 humidified chamber for 3 weeks. The medium was changed every 4 days. During the splitting/passaging of DPPSCs, cell density was maintained at 80–100 cells/cm^2 by detaching cells with 0.25% trypsin (Cellgro) and replating every 36–48 hours, when cells were 60% confluent.

DPPSC culture medium

The cell expansion medium consisted of 60% DMEM low glucose (Sigma) and 40% MCDB-201 (Sigma) supplemented with 1× Insulin-Transferrin-Selenium (ITS) (Sigma), 1× linoleic acid bovine serum albumin (LA-BSA) (Sigma), 10^{-9} M dexamethasone (Sigma), 10^{-4} M ascorbic acid 2-phosphate (Sigma), 100 units of penicillin, 1000 units of streptomycin (PAA), 2% foetal bovine serum (Sigma), 10 ng/ml hPDGF-BB (R&D Systems), 10 ng/ml EGF (R&D Systems), 1000 units/ml hLIF (Chemicon), Chemically Defined Lipid Concentrate (Gibco), 0.8 mg/ml BSA (Sigma) and 55 μM β-mercaptoethanol (β-ME, Sigma).

Base medium

The base medium consisted of 60% DMEM low glucose (Gibco), 40% MCDB-201 (Sigma) with 1× Insulin-Transferrin-Selenium, 1× linoleic acid BSA, 10^{-9} M dexamethasone (Sigma), 10^{-4} M ascorbic acid 2-phosphate (Sigma), 100 units of penicillin and 1000 units of streptomycin (Gibco).

Isolation and culture of human dental pulp mesenchymal stem cells (DPMSCs)

Human adult DPMSCs were isolated from the dental pulp of third molars and were suspended in Dulbecco's Modified Eagle's Medium (DMEM, Biochrom) containing 2 ng/ml basic fibroblast growth factor (bFGF) and 10% foetal bovine serum (FBS, Hyclone). Cells were plated at a density of 300,000 cells/cm^2. The medium was changed after 72 hours and every 2 days thereafter. To propagate DPMSCs, the cells were detached at 90% confluence by the addition of phosphate buffered saline (PBS, Biochrom) containing 0.05% trypsin-ethylenediaminetetraacetic acid (EDTA, Biochrom) and replated at a density of 4000 cells/cm^2.

Human NTERA-2 and IPS

NTERA-2 cells were obtained from the ATCC. Cells were maintained and cultured in Dulbecco's Modified Eagle's Medium supplemented with 10% foetal bovine serum and 1% penicillin-streptomycin at 37℃ humidified atmosphere at 5% CO_2. hIPS wire was kindly donated by our collaborators at the University of Navarra.

Flow cytometry

FACS analysis was carried out the same day of the extraction and again after two and three weeks of culture initiation. The following fluorochrome-labelled monoclonal antibodies were used: CD13 FITC (eBioscience), SSEA4 PE (eBioscience), OCT3/4 FITC (RD SYSTEMS), CD45 PE-Cy5 (BD Pharmingen), CD105 FITC (BD Pharmingen), CD34 PE-Cy5 (BD Pharmingen), CD73 PE (BD Pharmingen), CD146 FITC (BD Pharmingen), CD90 FITC (eBioscience), CD29 PE (BD Pharmingen), STRO1 FITC (BD Pharmingen), LIN28, SSEA1 PE, SOX2 PE and NANOG FITC (Abcam). For the analysis of control samples, different IgG isotypes coupled to FITC, PE and PE-Cy5 fluorochromes (BD Pharmingen) were used. The cell suspension (in PBS plus 2% FBS) was incubated for 45 minutes at 4℃ in the dark. Later, cells were washed twice with PBS containing 2% FBS and centrifuged for 6 minutes at 275 ***g*** (RCF). Depending on the number, cells were resuspended in 300 to 600 µl of PBS and 2% FBS. All flow cytometry measurements were made using a FACScan cytometer (FACSCalibur) and analysed using the winMDI 2.8 program.

Karyotyping

The cells were trypsinised and centrifuged at 250 ***g*** (RCF). The cell pellet was resuspended in a volume less than or equal to 500 µl of DMEM-LG and was then subjected to a hypotonic shock with 0.075 M KCl that had been pre-heated to 37℃ (the saline solution was added drop by drop under continuous agitation). After 30 minutes of incubation in the presence of KCl at 37℃, the cells were centrifuged at 300 ***g*** (RCF) for 10 minutes. The nucleus suspension was fixed twice consecutively in methanol:acetic acid (3:1). After the final centrifugation step, the final cell pellet was resuspended in fixation liquid and extensions were performed on glass slides that were pre-cooled to 4℃. The extensions were stained using GIEMSA stain and the number of cells in metaphase was counted using a light microscope at a 100× magnification with oil immersion. A minimum of 50 metaphases were counted per sample.

RNA isolation and qRT-PCR

Total cellular RNA samples were extracted using Trizol (Invitrogen) from the following cell types: DPPSCs at passages 5, 10 and 15 (P5, P10 and P15), H-NTERA, DPMSCs and differentiated cells. RNA was extracted weekly from the differentiated cells. Two µg of RNA was treated with DNase I (Invitrogen) and reverse-transcribed using M-MLV reverse transcriptase (Invitrogen). We analysed the efficacy of the cDNA (1, 0.1, 0.01, 0.001, 0.0001 dilutions) at different concentrations for all primers of pluripotent genes using NTERA cells as positive controls. Additionally, we tested the following samples as positive controls: hepatocyte markers from human liver cDNA samples, osteoblast markers from human bone cDNA and neuroectoderm markers from human brain cDNA (Ambion). Quantitative RT-PCR was performed using the CFX96 thermocycler (Bio-Rad). Quantitative RT-PCR was performed using 50 ng of cDNA and SYBR Green Supermix (Bio-Rad Laboratories, Inc.). cDNA samples were amplified using specific primers with the following conditions for 40 cycles. The expression levels of genes of interest (supplementary material Table S1) were normalised against the housekeeping gene *GAPDH*. The relative expression levels were normalised to human cDNAs (positive controls), which were assigned as 1. The results were analysed using the 2ΔΔCt method.

Western blotting

Total protein was extracted from the following samples: DPPSCs collected at different passages (P5, P10, P15 and P20), DPMSCs, NTERA-2, HEK 293 and bone marrow derived-MAPCs. Cell lysates with equal protein concentrations (20 µg/µl) were separated by SDS-PAGE on 12% polyacrylamide gels and transferred onto nitrocellulose membranes. The membranes were blocked with 1% (w/v) BSA in PBS containing 0.1% Tween 20, blotted with OCT3/4 and GAPDH primary antibodies (1:5000) and blotted with secondary antibodies (1:15,000). All antibodies were purchased from Abcam.

Immunofluorescence analysis

Samples were fixed with 4% paraformaldehyde (Sigma) for 4 minutes at room temperature followed by methanol (Sigma) for 2 minutes at −20℃. For nuclear ligands, cells were permeabilised with 0.1 M Triton X-100 (Sigma) for 10 minutes. Slides were incubated sequentially for 30 minutes each with primary antibody and FITC, PE or PE-Cy5-coupled anti-mouse IgG antibodies. Between each step, the slides were washed with 1% BSA (Sigma) in PBS. Cells were examined using confocal fluorescence microscopy (Confocal 1024 microscope, Olympus AX70, Olympus Optical, Tokyo).

Teratoma formation and histological analysis

Eight-week-old *nude* mice (Samtako Bio Korea, Seoul, Korea) were anaesthetised with diethyl ether. Fifty microliters of a P15 DPPSC or DPMSC cell suspension (4×10^7 cells/ml), from three different donors (14-, 17-, 28-year-old donors), mixed with 50 µl of Matrigel (BD) was injected subcutaneously into the dorsal flanks of the mice, which were then housed with free access to water and food under specific pathogen-free conditions. After 3 or 5 weeks, the teratoma-like structures were surgically dissected from the mice followed by fixation with 4% paraformaldehyde and 1.25% glutaraldehyde, and the mice were subjected to histological analysis. Specimens were embedded in paraffin, cut into 3 µm sections and stained with haematoxylin and eosin (H&E).

Immunohistochemistry

Samples were cut into 7-µm-thick sections for immunohistochemical staining. Slides were placed in PBS for 30 minutes to remove gelatin. After being washed twice with distilled water for 5 min, the sections were blocked against endogenous peroxidase in 0.3% hydrogen peroxide for 15 minutes and 10% normal goat serum in PBS for 1 hour at room temperature to reduce nonspecific antibody interactions. The slides were incubated with mouse monoclonal primary antibodies against human OCT3/4 (1:400, BD), NANOG (1:400, BD), SSEA4 (1:400, BD) and LIN28 (1:400, BD) at 4℃ overnight. After washing with PBS, the specimens were incubated with biotinylated goat anti-mouse secondary antibody (Zymed) and streptavidin peroxidase (Zymed) at room temperature for 10 minutes each. Finally, the specimens were visualised using a diaminobenzidine reagent kit (Zymed). The immunostained sections were counterstained with H&E.

Transmission electronic microscopy

A piece of the cell pellet measuring 1 mm^3 was fixed in a solution of 2% formaldehyde, 2.5% glutaraldehyde and Karnoski buffer with cacodylate (0.2 mol/l, pH 7.4). After 48 hours, the samples were soaked in araldite. The ultra-fine sections were stained for contrast with citrate and then observed using an electronic microscope (Zeiss EM900).

Scanning electron microscopy

For SEM analysis, samples were fixed in 2.5% glutaraldehyde (Ted Pella) in 0.1 M Na-cacodylate buffer (EMS, Electron Microscopy Sciences, Hatfield, PA) (pH 7.2) for 1 hour on ice. After fixation, the samples were treated with 1% osmium tetroxide (OsO_4) for 1 hour. The samples were dehydrated in serial solutions of acetone (30–100%) with the scaffolds mounted on aluminium stubs. The samples were then examined using a Zeiss 940 DSM scanning electron microscope.

Cell migration assay

The cell migration capacity of DPPSCs and DPMSCs from the same donor, as well as hNTERA cells, which were used as a positive control, was tested using a Multiscreen-MIC Plate polycarbonate filter (8 µM pore size) (Millipore). Approximately 1×10^3 cells in 150 µl were added to the bottom wells of the filter plate and incubated at 37℃ in 5% CO_2 for 6 hours. After incubation, the filters were removed and the topside of the membrane was scraped to remove non-migrated cells. The filters were then stained with Toluidine Blue. The cells were counted using a light microscope. Experiments were performed in triplicate and the data were pooled.

Short-chromosome genomic hybridisation (short-CGH)

DPPSCs were isolated one by one by manual catching and short-CGH technique was developed (Rius et al., 2010) ($n=15$). Hybridisation of control and DPPSC samples was carried out against a masculine cell preparation.

Mesoderm differentiation

For bone differentiation, cells were seeded in six-well plates and in a Cell Carrier 3D glass scaffold (Orla protein) on a 24-well plate with culture medium at a density of 3×10^3 cells P15 per cm^2. After 24 hours, differentiation was initiated by the following medium: α-MEM containing 10% heat inactivated FBS, 10 mM β-glycerol phosphate (Sigma), 50 µM of L-ascorbic acid (Sigma), 0.01 µM dexamethasone and 1% penicillin and streptomycin. The medium was changed every 3 days for 21 days. Differentiated cultures were evaluated by qRT-PCR for *ALP*, *OSTEONECTIN*, *OSTEOCALCIN*, *OSTEOPONTIN*, *COLLAGEN I*, *COLLAGEN III*, *BMP-2* and *NANOG* every week. The cultures were also analysed via immunofluorescence for OSTEOCALCIN and Alizarin Red staining after 3 weeks of differentiation.

Vessel-derived endothelial cell differentiation

Undifferentiated DPPSCs were cultured at a density of 3×10^3 cells per cm^2 with basal media for 1 day. Culture medium was then exchanged for differentiation media (Basal Media, FBS 2%, VEGF 50 ng/mL, bFGF 10 ng/ml). Cells were grown on coverslips and 6-well plates treated with Fibronectin and incubated at

37℃ at 5% CO_2. The medium was changed every 3 days for 21 days. Differentiated cultures were evaluated by qRT-PCR and immunofluorescence. RNA was obtained at day 0 and then weekly and tested for endothelial gene Flk1 and CD14 expression by qRT-PCR.

Endoderm differentiation

For 2D differentiation, DPPSCs P15 were seeded in 6-well plates with culture medium at a density of 5×10^4 cells/cm^2. The following day, the culture medium was exchanged for differentiation medium consisting of base medium containing 100 ng/ml HGF and 100 ng/ml FGF-4 (R&D Systems). The medium was changed every 3 days for 3 weeks. Differentiated cultures were evaluated by qRT-PCR for *GATA4*, *HNF3β*, *HNF6*, *AFP*, *ALB*, *CEBPA* and *NANOG* expression. Differentiated cells were identified using immunofluorescence microscopy for albumin protein expression and albumin secretion analysis at different days of differentiation.

For 3D differentiation, 5×10^4 cells P15 were seeded in a Cell Carrier 3D glass scaffold (Orla protein) pre-coated with 2% Matrigel and placed in 24-well plates with RPMI medium (Mediatech) supplemented with GlutaMAX and penicillin/streptomycin and containing 0.5% defined foetal bovine serum (FBS; HyClone) and 100 ng/ml Activin A (R&D Systems). Three days post-induction, the medium was refreshed using the same RPMI-based medium with 100 ng/ml Activin A but replacing FBS by KOSR 2%. After 2 days, definitive endoderm cultures were refreshed with RPMI medium supplemented with GlutaMAX and penicillin/streptomycin and containing 2% KOSR, 10 ng/ml FGF-4 (R&D Systems) and 10 ng/ml HGF (R&D Systems). Three days later, the cells were switched to minimal MDBK-MM medium (Sigma-Aldrich) supplemented with GlutaMAX and penicillin/streptomycin and containing 0.5 mg/ml bovine serum albumin (BSA) (Sigma-Aldrich), 10 ng/ml FGF-4 and 10 ng/ml HGF. After another 3 days, the cells were switched to complete hepatocyte culture medium (HCM) supplemented with SingleQuots (Lonza) and containing 10 ng/ml FGF-4, 10 ng/ml HGF, 10 ng/ml oncostatin M (R&D Systems) and 10^{-7} M dexamethasone (Sigma-Aldrich). Differentiation was continued for another 9 days. At each stage, the medium was refreshed every 2–3 days.

Neuroectoderm differentiation

For neural differentiation, cells P15 were seeded in 6-well plates and in 75 cm^2 flasks in base culture medium at a density of 3×10^3/cm^2. The following day, the culture medium was exchanged for differentiation medium; the differentiation medium differed from week to week. During the first week, the medium consisted of base medium and bFGF (100 ng/ml). During the second week, the medium consisted of base medium, FGF-8 (10 ng/ml) and SHH (100 ng/ml). During the third week, the medium consisted of base medium, BDNF (10 ng/ml) and GDNF (10 ng/ml) + N2 (R&D Systems). The medium was changed every 3 days. Neural differentiation was evaluated via qRT-PCR for *TAU*, *NURR1*, *NESTIN*, *GFAP*, *MBP*, *SOX1* and *NANOG* expression. Cultures were also analysed by immunofluorescence for PSD95-FITC and GALC-595 protein expression.

Alizarin Red staining

Cells were fixed in a 2.5% glutaraldehyde mixture that was freshly prepared in 1× PBS buffer for 10–15 minutes at room temperature. Cells were then washed with 1× PBS and 2% Alizarin Red solution (Millipore) was added to the fixed cells. Following incubation at 37℃ for 20 minutes, cells were then observed through microphotography (positively stained nodules are in orange-red).

Albumin secretion

The production of albumin was determined using the Albumin Assay Kit (Sigma) according to the manufacturer's instructions.

Alkaline phosphatase staining

For alkaline phosphatase (ALP) staining, EBs were fixed in a solution of 4% paraformaldehyde in PBS for 20 minutes. After extensive washing in PBS, cells were incubated in NTMT solution [10 mM NaCl, 100 mM Tris-HCl (pH 9), 50 mM $MgCl_2$, supplemented with 0.1% Tween-20] for 5 minutes and then in NTMT solution supplemented with NBT (Nitro-Blue Tetrazolium Chloride) and BCIP (5-Bromo-4-Chloro-3′-Indolyphosphate p-Toluidine Salt) in darkness until the staining developed.

ALP activity

During the 3D osteoblast differentiation of DPPSCs and from passage number 15, ALP activity was quantified every week by spectrophotometry using a Cromatest kit (Linear), in accordance with the manufacturer's instructions. We measured the absorbance of each sample at 1, 2, 3, 5 and 10 minutes.

Calcium quantification

Differentiated cells were washed twice with 1× PBS. Accumulated calcium was removed from the cellular components using lysis solutions contained in the Sigma kit for the analysis of calcium accumulation, according to the manufacturer's instructions. The total calcium was calculated using standard solutions and the absorbance was measured at 575 nm.

Cytochrome P450 3A4 metabolic activity assay

Cytochrome P450 (CYP) 3A4 enzyme activity assay was assessed by measurement of luciferase activity with the P450-Glo CYP3A4 assay, according to the manufacturer's instructions. Differentiated cells were incubated at 37℃ in DMSO plus ethanol supplemented with 50 µmol/l luciferin PFBE (150 µl/well) and without DMSO; undifferentiated DPPSCs were used as negative control. After 3 hours of incubation, 50 µl of medium was transferred in a 48-well plate and mixed with 50 µl of luciferin detection reagent to initiate luminescent reaction. After 20 minutes of incubation at room temperature, luminescence was measured with a Victor3 luminometer (PerkinElmer).

Statistical analysis

To assess the percentages of specific markers for DPPSCs, data were subjected to a regression analysis, which considered the independent variable (age) and the dependent variable (different markers). We established statistical significance at a P value less than 0.1 (90% confidence level). For all other data, the statistical test applied was the paired samples t-test, with statistical significance set at $P<0.05$. Data were analysed with SPSS Version 16.0 software. The values are expressed as the mean ± s.d.

Ethical regulations

Dental pulp tissues used for these experiments were obtained with informed consent from donors. All experiments were performed in accordance with the guidelines on human stem cell research issued by the Committee on Bioethics of the International University of Catalonia.

Acknowledgements

We thank M. Costa for help with FACS analysis, as well as J. Navarro and J. del Rey for their dedication in cytogenetic analysis using a newly developed CGH technique was performed in the Unitat de Biologia Cellular i Genètica Mèdica Eugin-UAB. In memory of Nuria Durany, without whom this article would not have been possible. Author contributions were as follows: A.M., conception and design, collection and assembly of data, data analysis and interpretation, manuscript writing and final approval of the manuscript; C.G.-R., collection and assembly of data and manuscript writing; M.F., collection and assembly of data; D.G.-F., collection and assembly of data; M.B., data analysis and interpretation; M.C., collection and assembly of data; H.-S.J, financial support, administrative support, data analysis and interpretation; F.H.-A., provision of study patients; N.C., data analysis and interpretation; F.P., administrative support, and data analysis and interpretation; E.F.P., provision of study patients; L.G., financial support, administrative support and final approval of manuscript.

Funding

The Universitat International de Catalunya supported all this work. This research received no specific grant from any funding agency in the public, commercial or not-for-profit sectors.

Supplementary material available online at
http://jcs.biologists.org/lookup/suppl/doi:10.1242/jcs.096537/-/DC1

References

About, I., Bottero, M. J., de Denato, P., Camps, J., Franquin, J. C. and Mitsiadis, T. A. (2000). Human dentin production in vitro. *Exp. Cell Res.* **258**, 33-41.

Arthur, A., Rychkov, G., Shi, S., Koblar, S. A. and Gronthos, S. (2008). Adult human dental pulp stem cells differentiate toward functionally active neurons under appropriate environmental cues. *Stem Cells* **26**, 1787-1795.

Atari, M., Barajas, M., Hernández-Alfaro, F., Gil, C., Fabregat, M., Ferrés Padró, E., Giner, L. and Casals, N. (2011). Isolation of pluripotent stem cells from human third molar dental pulp. *Histol. Histopathol.* **26**, 1057-1070.

Atari, M., Caballé-Serrano, J., Gil-Recio, C., Giner-Delgado, C., Martínez-Sarrà, E., García-Fernández, D. A., Barajas, M., Hernández-Alfaro, F., Ferrés-Padró, E. and Giner-Tarrida, L. (2012). The enhancement of osteogenesis through the use of dental pulp pluripotent stem cells in 3D. *Bone* **50**, 930-941.

Benton, G., George, J., Kleinman, H. K. and Arnaoutova, I. P. (2009). Advancing science and technology via 3D culture on basement membrane matrix. *J. Cell. Physiol.* **221**, 18-25.

Braccini, A., Wendt, D., Jaquiery, C., Jakob, M., Heberer, M., Kenins, L., Wodnar-Filipowicz, A., Quarto, R. and Martin, I. (2005). Three-dimensional perfusion culture of human bone marrow cells and generation of osteoinductive grafts. *Stem Cells* **23**, 1066-1072.

Casagrande, L., Mattuella, L. G., de Araujo, F. B. and Eduardo, J. (2006). Stem cells in dental practice: perspectives in conservative pulp therapies. *J. Clin. Pediatr. Dent.* **31**, 25-27.

Cheng, P. H., Snyder, B., Fillos, D., Ibegbu, C. C., Huang, A. H. and Chan, A. W. (2008). Postnatal stem/progenitor cells derived from the dental pulp of adult chimpanzee. *BMC Cell Biol.* **9**, 20.

Cordeiro, M. M., Dong, Z., Kaneko, T., Zhang, Z., Miyazawa, M., Shi, S., Smith, A. J. and Nör, J. E. (2008). Dental pulp tissue engineering with stem cells from exfoliated deciduous teeth. *J. Endod.* **34**, 962-969.

d'Aquino, R., Graziano, A., Sampaolesi, M., Laino, G., Pirozzi, G., De Rosa, A. and Papaccio, G. (2007). Human postnatal dental pulp cells co-differentiate into osteoblasts and endotheliocytes: a pivotal synergy leading to adult bone tissue formation. *Cell Death Differ.* **14**, 1162-1171.

Dezawa, M., Ishikawa, H., Hoshino, M., Itokazu, Y. and Nabeshima, Y. (2005). Potential of bone marrow stromal cells in applications for neuro-degenerative, neuro-traumatic and muscle degenerative diseases. *Curr. Neuropharmacol.* **3**, 257-266.

Dhawan, A., Strom, S. C., Sokal, E. and Fox, I. J. (2010). Human hepatocyte transplantation. *Methods Mol. Biol.* **640**, 525-534.

Ebert, A. D., Yu, J., Rose, F. F., Jr, Mattis, V. B., Lorson, C. L., Thomson, J. A. and Svendsen, C. N. (2009). Induced pluripotent stem cells from a spinal muscular atrophy patient. *Nature* **457**, 277-280.

Fuchs, E. and Segre, J. A. (2000). Stem cells: a new lease on life. *Cell* **100**, 143-155.

Fujii, S., Maeda, H., Wada, N., Tomokiyo, A., Saito, M. and Akamine, A. (2008). Investigating a clonal human periodontal ligament progenitor/stem cell line in vitro and in vivo. *J. Cell. Physiol.* **215**, 743-749.

Gandia, C., Armiñan, A., García-Verdugo, J. M., Lledó, E., Ruiz, A., Miñana, M. D., Sanchez-Torrijos, J., Payá, R., Mirabet, V., Carbonell-Uberos, F. et al. (2008). Human dental pulp stem cells improve left ventricular function, induce angiogenesis, and reduce infarct size in rats with acute myocardial infarction. *Stem Cells* **26**, 638-645.

Gay, I. C., Chen, S. and MacDougall, M. (2007). Isolation and characterization of multipotent human periodontal ligament stem cells. *Orthod. Craniofac. Res.* **10**, 149-160.

Gronthos, S., Mankani, M., Brahim, J., Robey, P. G. and Shi, S. (2000). Postnatal human dental pulp stem cells (DPSCs) in vitro and in vivo. *Proc. Natl. Acad. Sci. USA* **97**, 13625-13630.

Hanna, J. H., Saha, K. and Jaenisch, R. (2010). Pluripotency and cellular reprogramming: facts, hypotheses, unresolved issues. *Cell* **143**, 508-525.

Harada, H., Kettunen, P., Jung, H. S., Mustonen, T., Wang, Y. A. and Thesleff, I. (1999). Localization of putative stem cells in dental epithelium and their association with Notch and FGF signaling. *J. Cell Biol.* **147**, 105-120.

He, F., Yang, Z., Tan, Y., Yu, N., Wang, X., Yao, N. and Zhao, J. (2009). Effects of Notch ligand Delta1 on the proliferation and differentiation of human dental pulp stem cells in vitro. *Arch. Oral Biol.* **54**, 216-222.

Hirata, T. M., Ishkitiev, N., Yaegaki, K., Calenic, B., Ishikawa, H., Nakahara, T., Mitev, V., Tanaka, T. and Haapasalo, M. (2010). Expression of multiple stem cell markers in dental pulp cells cultured in serum-free media. *J. Endod.* **36**, 1139-1144.

Honda, M. J., Fong, H., Iwatsuki, S., Sumita, Y. and Sarikaya, M. (2008). Tooth-forming potential in embryonic and postnatal tooth bud cells. *Med. Mol. Morphol.* **41**, 183-192.

Huo, N., Tang, L., Yang, Z., Qian, H., Wang, Y., Han, C., Gu, Z., Duan, Y. and Jin, Y. (2010). Differentiation of dermal multipotent cells into odontogenic lineage induced by embryonic and neonatal tooth germ cell-conditioned medium. *Stem Cells Dev.* **19**, 93-104.

Illich, D. J., Demir, N., Stojković, M., Scheer, M., Rothamel, D., Neugebauer, J., Hescheler, J. and Zöller, J. E. (2011). Concise review: induced pluripotent stem cells and lineage reprogramming: prospects for bone regeneration. *Stem Cells* **29**, 555-563.

Iohara, K., Nakashima, M., Ito, M., Ishikawa, M., Nakasima, A. and Akamine, A. (2004). Dentin regeneration by dental pulp stem cell therapy with recombinant human bone morphogenetic protein 2. *J. Dent. Res.* **83**, 590-595.

Itskovitz-Eldor, J., Schuldiner, M., Karsenti, D., Eden, A., Yanuka, O., Amit, M., Soreq, H. and Benvenisty, N. (2000). Differentiation of human embryonic stem cells into embryoid bodies compromising the three embryonic germ layers. *Mol. Med.* **6**, 88-95.

Laino, G., d'Aquino, R., Graziano, A., Lanza, V., Carinci, F., Naro, F., Pirozzi, G. and Papaccio, G. (2005). A new population of human adult dental pulp stem cells: a useful source of living autologous fibrous bone tissue (LAB). *J. Bone Miner. Res.* **20**, 1394-1402.

Laino, G., Carinci, F., Graziano, A., d'Aquino, R., Lanza, V., De Rosa, A., Gombos, F., Caruso, F., Guida, L., Rullo, R. et al. (2006). In vitro bone production using stem cells derived from human dental pulp. *J. Craniofac. Surg.* **17**, 511-515.

Leeb, C., Jurga, M., McGuckin, C., Moriggl, R. and Kenner, L. (2010). Promising new sources for pluripotent stem cells. *Stem Cell Rev.* **6**, 15-26.

Liu, H., Gronthos, S. and Shi, S. (2006). Dental pulp stem cells. *Methods Enzymol.* **419**, 99-113.

Maltman, D. J. and Przyborski, S. A. (2010). Developments in three-dimensional cell culture technology aimed at improving the accuracy of in vitro analyses. *Biochem. Soc. Trans.* **38**, 1072-1075.

Martin, G. R. and Evans, M. J. (1975). Differentiation of clonal lines of teratocarcinoma cells: formation of embryoid bodies in vitro. *Proc. Natl. Acad. Sci. USA* **72**, 1441-1445.

Mina, M. and Braut, A. (2004). New insight into progenitor/stem cells in dental pulp using Col1a1-GFP transgenes. *Cells Tissues Organs (Print)* **176**, 120-133.

Miura, M., Gronthos, S., Zhao, M., Lu, B., Fisher, L. W., Robey, P. G. and Shi, S. (2003). SHED: stem cells from human exfoliated deciduous teeth. *Proc. Natl. Acad. Sci. USA* **100**, 5807-5812.

Morsczeck, C., Frerich, B. and Driemel, O. (2009). Dental stem cell patents. *Recent Pat. DNA Gene Seq.* **3**, 39-43.

Noël, D., Djouad, F. and Jorgense, C. (2002). Regenerative medicine through mesenchymal stem cells for bone and cartilage repair. *Curr. Opin. Investig. Drugs* **3**, 1000-1004.

Nosrat, I. V., Widenfalk, J., Olson, L. and Nosrat, C. A. (2001). Dental pulp cells produce neurotrophic factors, interact with trigeminal neurons in vitro, and rescue motoneurons after spinal cord injury. *Dev. Biol.* **238**, 120-132.

O'Connor, M. D., Kardel, M. D., Iosfina, I., Youssef, D., Lu, M., Li, M. M., Vercauteren, S., Nagy, A. and Eaves, C. J. (2008). Alkaline phosphatase-positive colony formation is a sensitive, specific, and quantitative indicator of undifferentiated human embryonic stem cells. *Stem Cells* **26**, 1109-1116.

Oda, Y., Yoshimura, Y., Ohnishi, H., Tadokoro, M., Katsube, Y., Sasao, M., Kubo, Y., Hattori, K., Saito, S., Horimoto, K. et al. (2010). Induction of pluripotent stem cells from human third molar mesenchymal stromal cells. *J. Biol. Chem.* **285**, 29270-29278.

Otaki, S., Ueshima, S., Shiraishi, K., Sugiyama, K., Hamada, S., Yorimoto, M. and Matsuo, O. (2007). Mesenchymal progenitor cells in adult human dental pulp and their ability to form bone when transplanted into immunocompromised mice. *Cell Biol. Int.* **31**, 1191-1197.

Papapetrou, E. P., Tomishima, M. J., Chambers, S. M., Mica, Y., Reed, E., Menon, J., Tabar, V., Mo, Q., Studer, L. and Sadelain, M. (2009). Stoichiometric and temporal requirements of Oct4, Sox2, Klf4, and c-Myc expression for efficient human iPSC induction and differentiation. *Proc. Natl. Acad. Sci. USA* **106**, 12759-12764.

Peters, H. and Balling, R. (1999). Teeth. Where and how to make them. *Trends Genet.* **15**, 59-65.

Ratajczak, M. Z., Zuba-Surma, E. K., Machalinski, B., Ratajczak, J. and Kucia, M. (2008). Very small embryonic-like (VSEL) stem cells: purification from adult organs, characterization, and biological significance. *Stem Cell Rev.* **4**, 89-99.

Rius, M., Obradors, A., Daina, G., Cuzzi, J., Marquès, L., Calderón, G., Velilla, E., Martínez-Passarell, O., Oliver-Bonet, M., Benet, J. et al. (2010). Reliability of short comparative genomic hybridization in fibroblasts and blastomeres for a comprehensive aneuploidy screening: first clinical application. *Hum. Reprod.* **25**, 1824-1835.

Rizzino, A. (2009). Sox2 and Oct-3/4: a versatile pair of master regulators that orchestrate the self-renewal and pluripotency of embryonic stem cells. *Wiley Interdiscip. Rev. Syst. Biol. Med.* **1**, 228-236.

Sloan, A. J. and Smith, A. J. (2007). Stem cells and the dental pulp: potential roles in dentine regeneration and repair. *Oral Dis.* **13**, 151-157.

Smith, K. P., Luong, M. X. and Stein, G. S. (2009). Pluripotency: toward a gold standard for human ES and iPS cells. *J. Cell. Physiol.* **220**, 21-29.

Stevens, A., Zuliani, T., Olejnik, C., LeRoy, H., Obriot, H., Kerr-Conte, J., Formstecher, P., Bailliez, Y. and Polakowska, R. R. (2008). Human dental pulp stem cells differentiate into neural crest-derived melanocytes and have label-retaining and sphere-forming abilities. *Stem Cells Dev.* **17**, 1175-1184.

Takahashi, K. and Yamanaka, S. (2006). Induction of pluripotent stem cells from mouse embryonic and adult fibroblast cultures by defined factors. *Cell* **126**, 663-676.

Téclès, O., Laurent, P., Zygouritsas, S., Burger, A. S., Camps, J., Dejou, J. and About, I. (2005). Activation of human dental pulp progenitor/stem cells in response to odontoblast injury. *Arch. Oral Biol.* **50**, 103-108.

Thesleff, I. and Aberg, T. (1999). Molecular regulation of tooth development. *Bone* **25**, 123-125.

Undale, A. H., Westendorf, J. J., Yaszemski, M. J. and Khosla, S. (2009). Mesenchymal stem cells for bone repair and metabolic bone diseases. *Mayo Clin. Proc.* **84**, 893-902.

Verfaillie, C. M. (2005). Multipotent adult progenitor cells: an update. *Novartis Found Symp.* **265**, 55-61.

Volponi, A. A., Pang, Y. and Sharpe, P. T. (2010). Stem cell-based biological tooth repair and regeneration. *Trends Cell Biol.* **20**, 715-722.

Yang, X., van der Kraan, P. M., van den Dolder, J., Walboomers, X. F., Bian, Z., Fan, M. and Jansen, J. A. (2007). STRO-1 selected rat dental pulp stem cells transfected with adenoviral-mediated human bone morphogenetic protein 2 gene show enhanced odontogenic differentiation. *Tissue Eng.* **13**, 2803-2812.

Yu, J., Vodyanik, M. A., Smuga-Otto, K., Antosiewicz-Bourget, J., Frane, J. L., Tian, S., Nie, J., Jonsdottir, G. A., Ruotti, V., Stewart, R. et al. (2007). Induced pluripotent stem cell lines derived from human somatic cells. *Science* **318**, 1917-1920.

Zhang, W., Walboomers, X. F., Wolke, J. G., Bian, Z., Fan, M. W. and Jansen, J. A. (2005). Differentiation ability of rat postnatal dental pulp cells in vitro. *Tissue Eng.* **11**, 357-368.

Zhang, W., Walboomers, X. F., Shi, S., Fan, M. and Jansen, J. A. (2006a). Multilineage differentiation potential of stem cells derived from human dental pulp after cryopreservation. *Tissue Eng.* **12**, 2813-2823.

Zhang, W., Walboomers, X. F., van Kuppevelt, T. H., Daamen, W. F., Bian, Z. and Jansen, J. A. (2006b). The performance of human dental pulp stem cells on different three-dimensional scaffold materials. *Biomaterials* **27**, 5658-5668.

Zuba-Surma, E. K., Kucia, M., Ratajczak, J. and Ratajczak, M. Z. (2009). "Small stem cells" in adult tissues: very small embryonic-like stem cells stand up! *Cytometry A* **75**, 4-13.

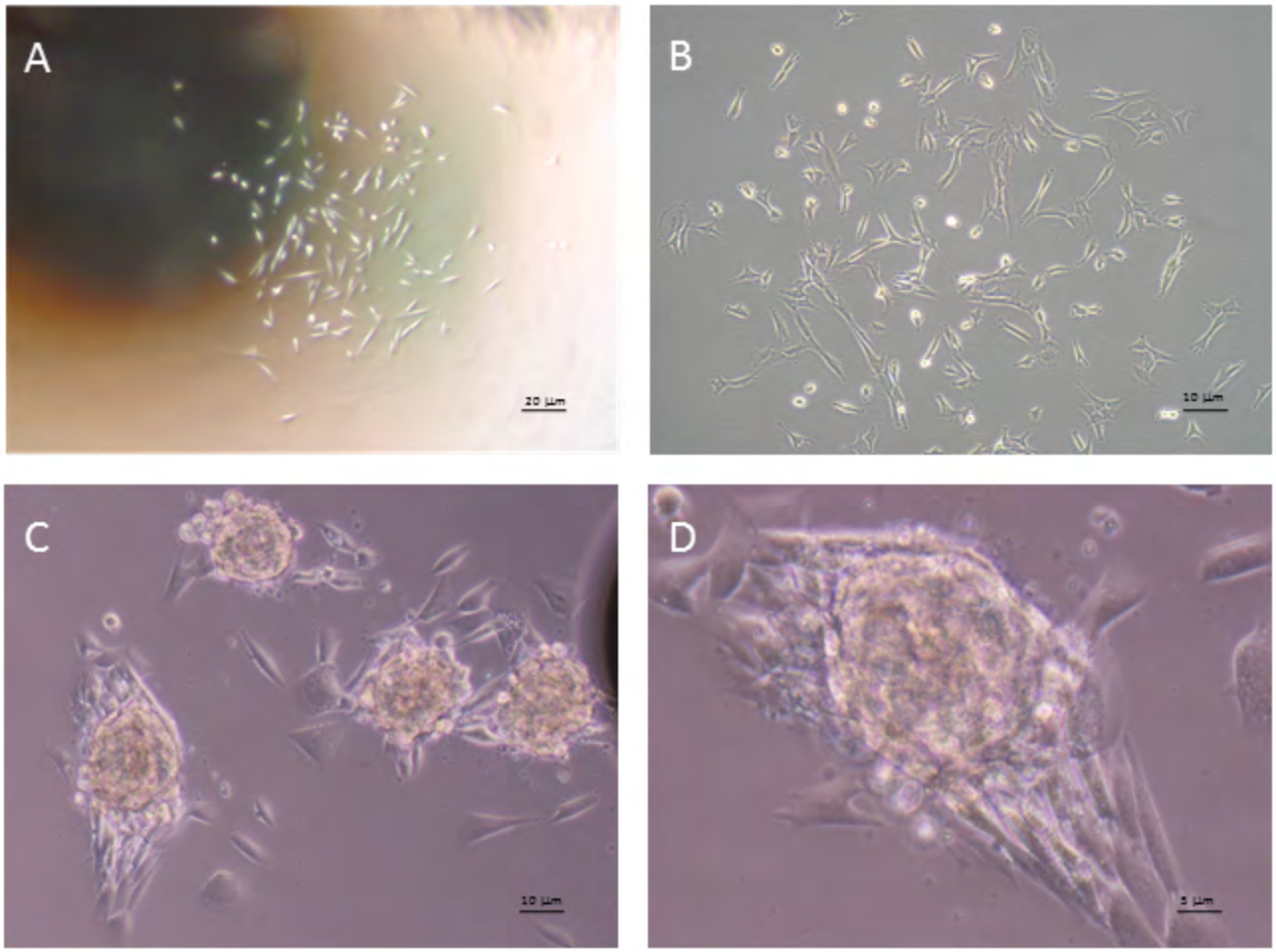

Fig. S1. Images of DPPSCs colonies. Colony formation was observed specially when the cells were cultured by the hanging drop method. When colonies were seeded into adherent surfaces cells tended to migrate.

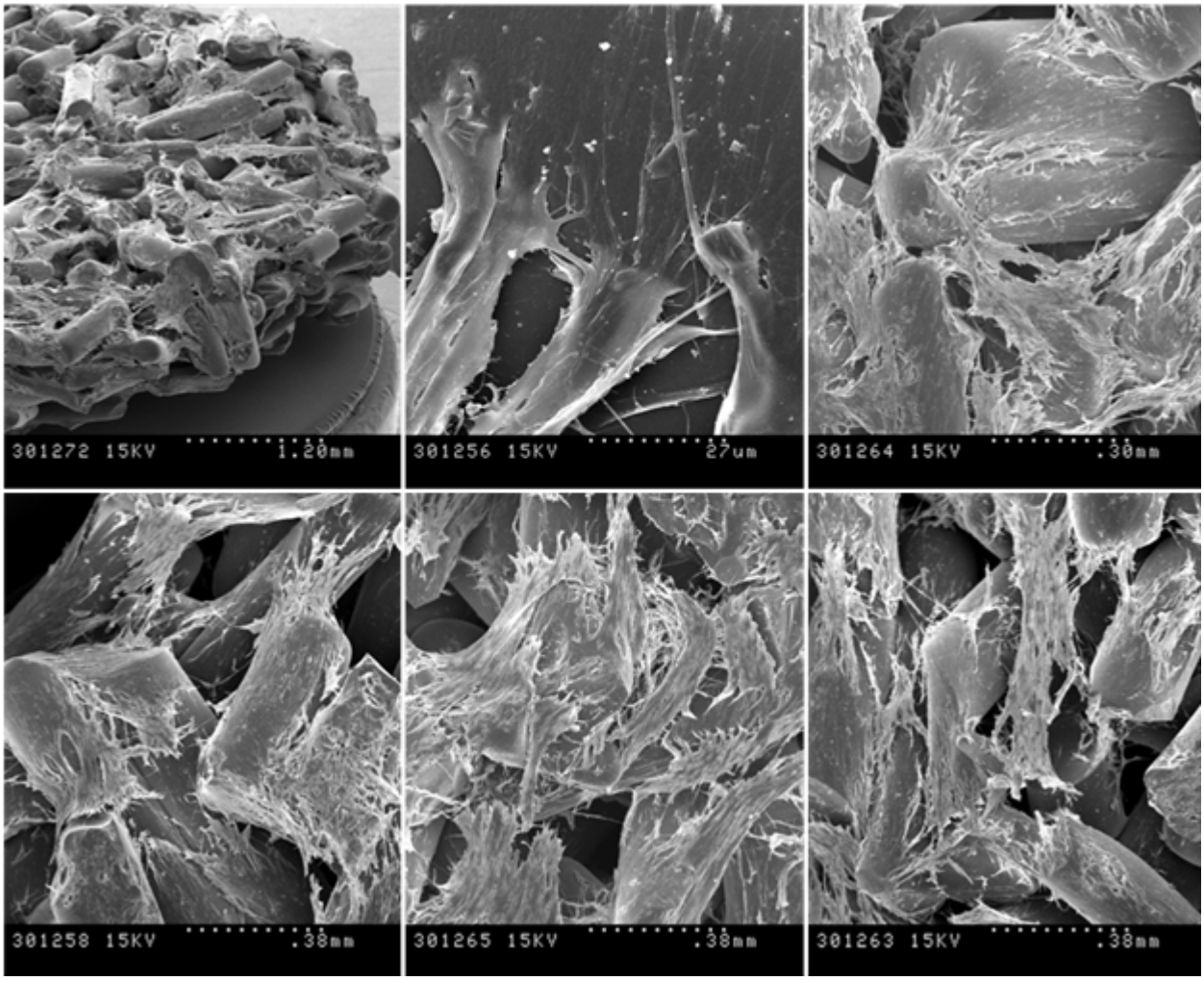

Fig. S2. Images from the SEM of DPPSCs seeded in the Cell Carrier 3D glass scaffold.

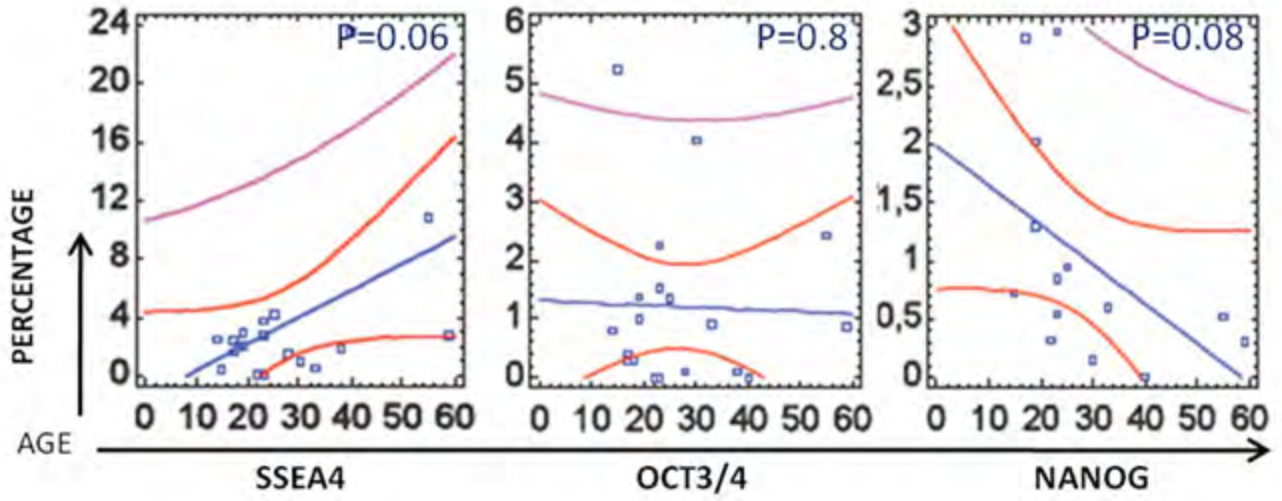

Fig. S3. Correlation between age and percentage of expression of embryonic markers in dental pulps extracted from patients with different ages.

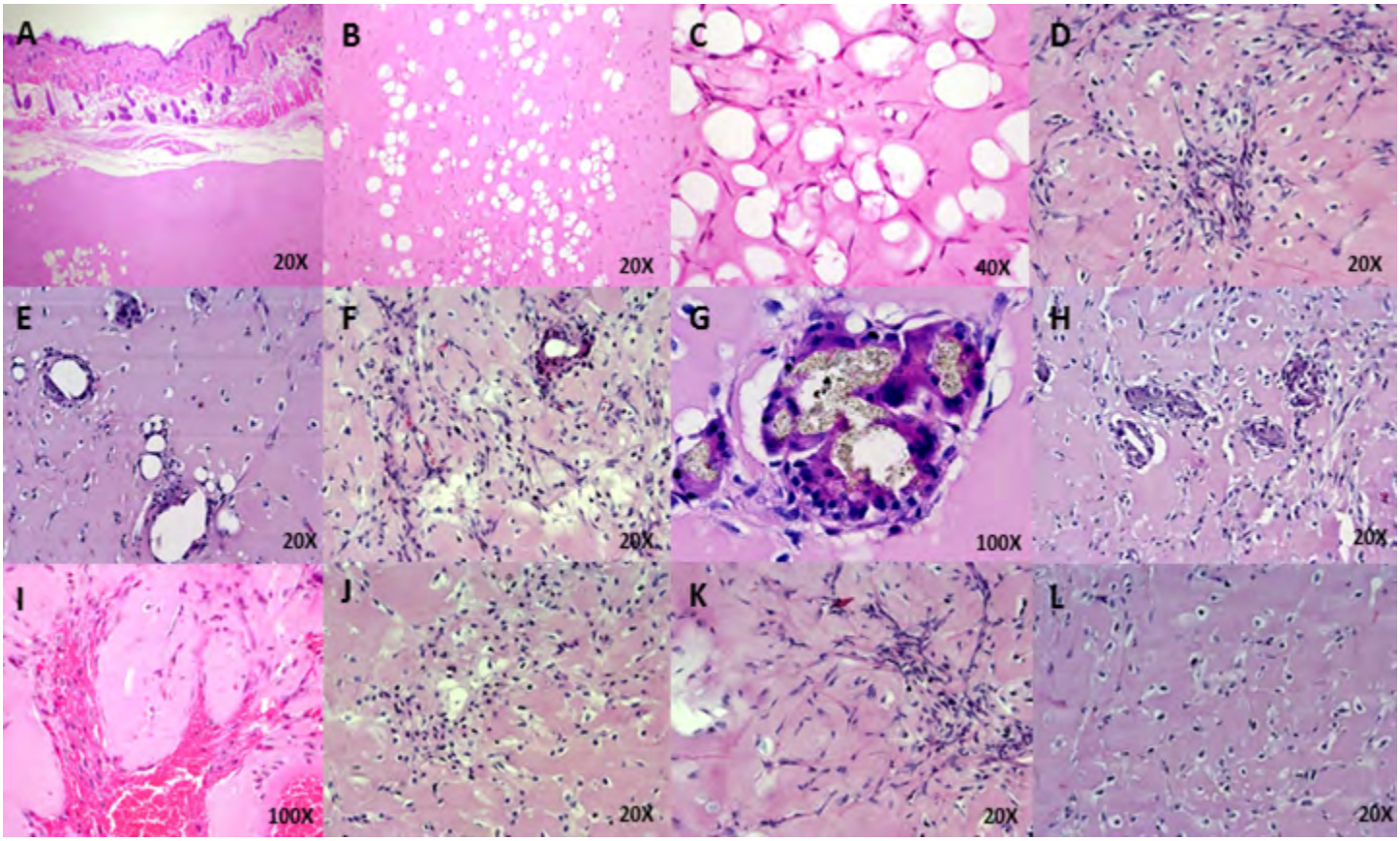

Fig. S4. Teratoma-like formation 5 weeks after of injection of DPPSCs into nude mice. showed the formation of multiple adult structures with origins in different embryonic layers, such as chondroid tissue, chondroid matrix, fibroblasts and collagen fibres, adipose tissue and endothelium (mesoderm A-D), gut-like epithelium (endoderm, E-H), and neural-like tissue such as nerve and keratin (ectoderm, I-L), (n=3, from 14, 17, 28 years old donors).

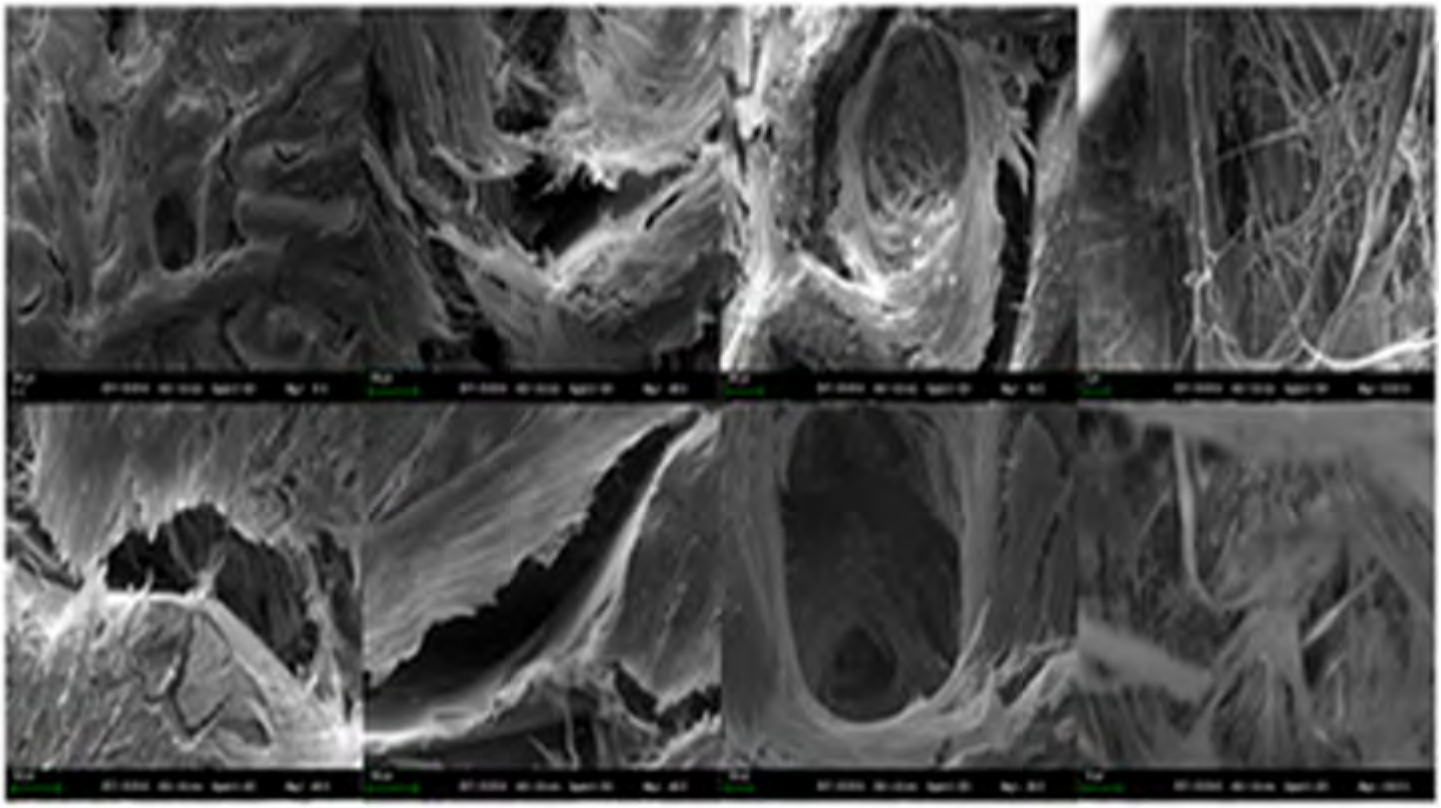

Fig. S5. Images from the SEM analysis of DPPSCs induced into osteogenic differentiation after 3 weeks.

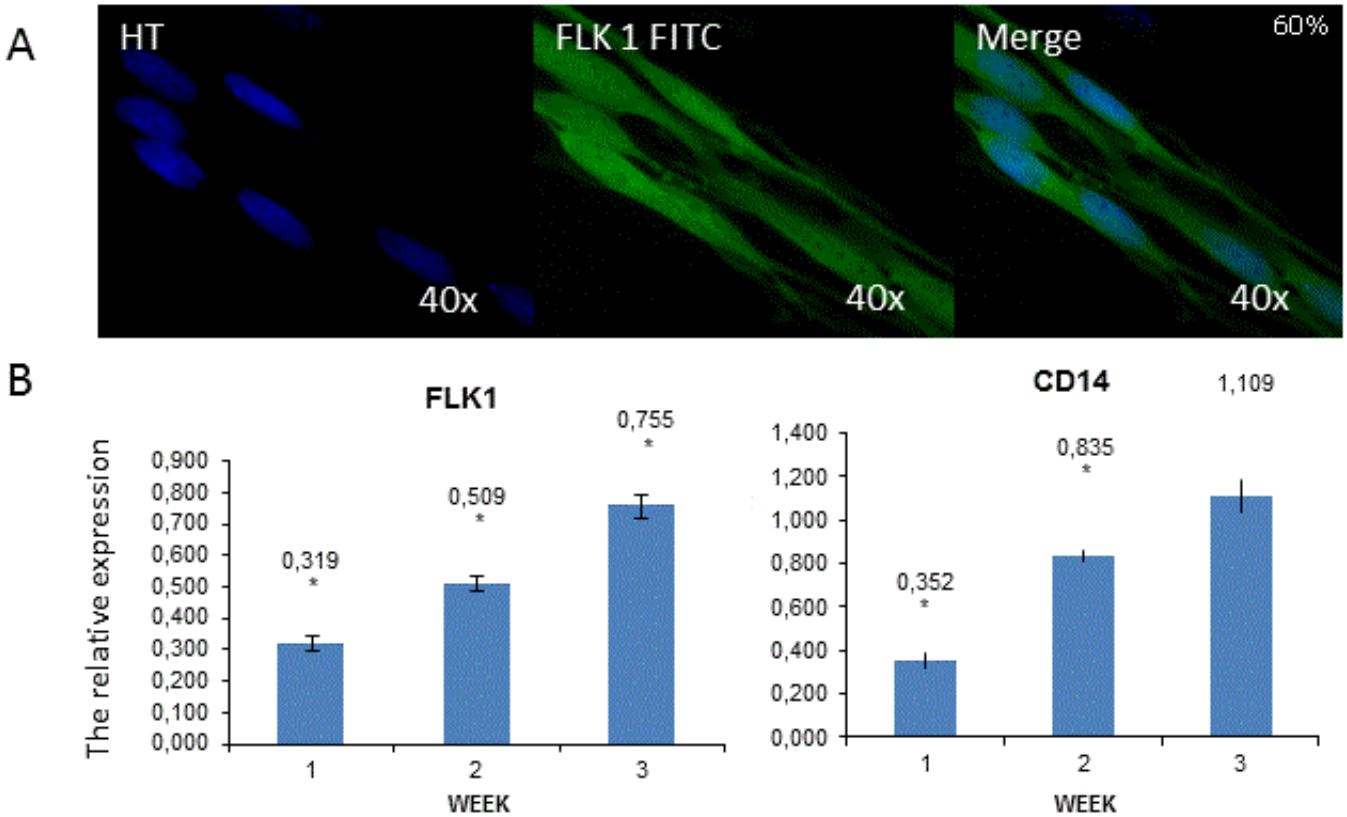

Fig. S6. A: Immunofluorescence analysis of FLK1 FITC for cells differentiated into endothelium. **B**: FLK1 and CD14 detection by qRT-PCR at different time points during differentiation of DPPSCs (n=3, **P*<0.05). mRNA levels were normalised to GAPDH (a housekeeping gene). The relative expression was normalised to Day 0 cDNAs, which is normalised to 0.

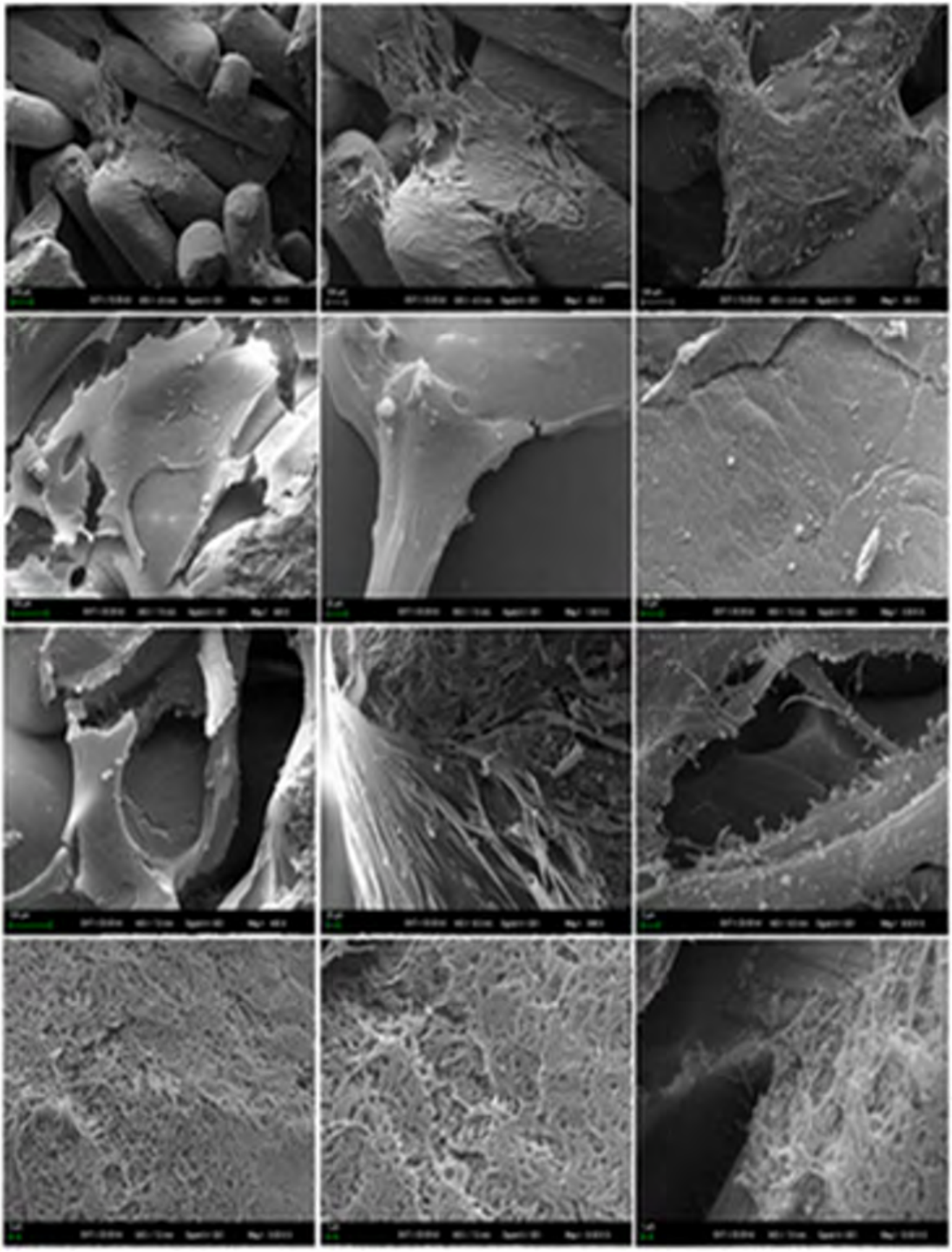

Fig. S7. Images from the SEM analysis of DPPSCs induced into hepatic differentiation after 3 weeks.

Gene	Forward	Reverse
OCT3/4	GACAGGGGGAGGGGAGGAGCTAGG	CTTCCCTCCAACCAGTTGCCCCAAAC
SOX2	GGGAAATGGGAGGGGTGCAAAAGAGG	TTGCGTGAGTGTGGATGGGATTGGTG
NANOG	AAAGAATCTTCACCTATGCC	GAAGGAAGAGGAGAGACAGT
GAPDH	TGGAGCTTCAGAAGCTCAACACCA	CCTGACCATGAGTCTGTTGCTCTA
TERT	CCTGCTCAAGCTGACTCGACACCG	GGAAAAGCTGGCCCTGGGGTGGAG
ALP	GAAGGTGAAGGTCGGAGTCA	TGGACTCCACGACGTACTCA
OSTEOCALCIN	GGTGCAGAGTCCAGCAAAGG	AGCGCCTGGGTCTCTTCCTA
COLLAGEN I	CCCTGGAAAGAATGGAGATCGAT	ACTGAAACCTCTGTGTCCCTTCA
GATA4	TCCCTCTTCCCTCCTCAAAT	TTCCCCTAACCAGATTGTCG
HNF3B	ATTGCTGGTCGTTTGTTGTG	TACGTGTTCATGCCGTTCAT
HNF6	CTTAGCAGCATGCAAAAGGA	TGCGTTCATGAAGAAGTTGC
ALB	GCACAGAATCCTTGGTGAACAG	ATGGAAGGTGAATGTTTCAGCA
AFP	CCCGAACTTTCCAAGCCATA	TACATGGGCCACATCCAGG
CYP3A4	GCCTGGTGCTCCTCTATCTA	GGCTGTTGACCATCATAAAAG
NURR1	GCTGTTGGGATGGTCAAAGAAG	GGTTTCGAGGGCAAACGA
TAU	TCCAGTCGAAGATTGGGTCC	GCTTGTGGGTTTCAATCTTTTTATTT
NESTIN	CAGGAGAAACAGGGCCTACA	TGGGAGCAAAGATCCAAGAC
OSTEOPONTIN	CTCAGGCCAGTTGCAGCC	CAAAAGCAAATCACTGCAATTCTC
COLLAGEN III	GGGAACAACTTGATGGTGCT	CCTCCTTCAACAGCTTCCTG
BMP2	AACACTGTGCGCAGCTTCC	CTCCGGGTTGTTTTCCCAC
CEBPA	ACAAGAACAGCAACGAGTACCG	CATTGTCACTGGTCAGCTCCA
MBP	AGGGATTCAAGGGAGTCGAT	GTGGGTTTTCAGCGTCTAGC
SOX1	AAGATGCACAACTCGGAGATCAG	TGTAATCCGGGTGTTCCTTCAT
GFAP	CCGTGCAGACCTTCTCCAAC	GGCCTTCTGACACAGACTTGGT
MIXL1	CAGAACAGGCGTGCCAAGTC	TTCCAGGAGCACAGTGGTTGA
GATA6	AATGACTCCAGAACAACAACTGGG	CTCCCTCCAGTCCCATCAGC

Table S1. Primers used for amplification.

	DPPSC				DPMSC		
	P5	P10	P15		P5	P10	P15
CD45 *	0,066	0,02	0,019	CD45 *	0,036	0,036	0,01
CD146	5	8	12	CD146	0,2	0,2	0,2
CD105 **	85,2	86,4	92,6	CD105 *	62	67	67
CD90 *	11,2	12,6	17,2	CD90 **	28,2	78	15,6
CD73	28,4	29,2	25,4	CD73 *	72	67,6	67,6
CD13 *	86,8	83,4	93,6	CD13*	81,2	82,8	82,8
CD34 *	0,00002	0,00002	0,006	CD34 *	0,002	0,002	0,002
STRO-1	8,8	8,8	4,54	STRO-1 *	47,4	72,8	72,8
LIN28	7	12	22,8	LIN28	0,43	0,36	0,3
SSEA4 *	5,8	13,2	42,4	SSEA4 *	0,0028	0,0182	0,0182
SOX2	4,4	8,6	17,8	SOX2	0,0002	0	0
NANOG	8,6	14,2	25,6	NANOG	0,5	0,34	0,14
OCT3/4 *	23,2	39	57	OCT3/4 *	0,36	0,16	0,07
OCT3/4+SSEA4 *	11	15	18	OCT3/4+SSEA4 *	0,001	0,19	0,001

Table S2. Comparison of expression of different markers between DPPSCs and DPMSCs isolated from the same donors (n=5) at different passages. Expressed in %. *P≤0.05, **P≤0.001.

		OCT3/4			NANOG			CD73			
FSC Interval	Gate	% Gated	% Total	Gated Events	% Gated	% Total	Gated Events	% Gated	% Total	Gated Events	Gate
-	-	98.55	98.55	6062	97.81	97.81	6132	77.86	77.86	14649	-
400-500	G1	99.63	4.49	273	99.60	4.09	252	69.05	1.78	378	G7
500-600	G2	99.94	27.05	1641	99.88	26.19	1608	87.99	11.05	1840	G8
600-700	G3	100.00	33.07	2005	99.90	33.35	2047	90.49	23.05	3732	G9
700-800	G4	100.00	17.02	1032	100.00	16.47	1010	91.22	20.21	3246	G10
800-900	G5	100.00	6.71	407	100.00	6.72	412	93.91	9.68	1510	G11
900-1000	G6	100.00	3.48	211	100.00	3.67	225	95.31	3.33	512	G12
SSC Interval	Gate	% Gated	% Total	Gated Events	% Gated	% Total	Gated Events	% Gated	% Total	Gated Events	Gate
-	-	98.81	98.81	6062	97.64	97.64	6132	78.55	78.55	14649	-
200-300	G1	99.77	7.13	433	99.79	7.73	475	90.22	1.39	225	G9
300-400	G2	99.93	23.24	1410	100.00	22.34	1370	89.59	12.81	2095	G10
400-500	G3	100.00	25.12	1523	99.94	25.59	1570	90.98	19.07	3070	G11
500-600	G4	100.00	15.19	921	99.89	14.89	914	90.57	15.41	2493	G12
600-700	G5	99.82	9.24	561	99.82	8.82	542	91.52	9.14	1463	G13
700-800	G6	100.00	4.32	262	100.00	4.42	271	93.15	5.01	788	G14
800-900	G7	100.00	3.94	239	100.00	3.33	204	96.45	2.78	422	G15
900-1000	G8	100.00	2.59	157	100.00	2.30	141	96.36	1.62	247	G16

Table S3. Data obtained from FACS. Expression of OCT3/4, NANOG and CD73 in different ranges of FSC and SSC.

AGE	Nolla stages	OCT3/4	NANOG
8	6	1.39	3.9
9	6	1.71	3.8
11	7	1.07	1.83
11	7	1.50	1.74
12	8	1.61	2.10
13	8	1.41	1.97
14	9	0.84	0.81
17	9	0.37	0.62
18	9	0.34	0.84
19	10	1.37	2.02
19	10	0.98	1.29
22	10	0.71	0.31
23	10	0.51	2.97
23	10	1.53	0.84

Table S4. Correlation between age, nolla stages and expression of embryonic markers (N=14).

Gene	Day 0	Week 1	Week 2	Week 3
Osteopontin	0	1.9, 2.6, 3.4	3.1, 4.2, 5.4	0.98, 1.01, 0.7
Collagen I	0	2.08, 3.4, 5.6	5.04, 6.71, 9.14	11.2, 14.84, 18.4
Collagen III	0	1.07, 3.02, 3.71	6.72, 5.85, 8.44	9.81, 8.25, 14.01
BMP-2	0	0.92, 1.45, 2.61	3.04, 4.94, 6.41	6.01, 8.12, 10.02
NANOG	1.84, 1.89, 1.61	0.7, 0.42, 0.41	0.14, 0.09. 0.08	0, 0, 0.02

Table S5. Quantitative RT-PCR (*OSTEOPONTIN*, *COLLAGEN I*, *COLLAGEN III*, *BMP2*, and *NANOG*) of mesoderm differentiation markers. mRNA levels were analysed on day 0 and weeks 1, 2 and 3 of DPPSC differentiation into bone-like cells (n=3). mRNA levels were normalised to the housekeeping gene *GAPDH* and compared with levels in human bone cDNAs.

Gene	Day 0	Week 1	Week 2	Week 3
AFP	0	0,25. 0,31. 0,54	0,51, 0,61. 0,71	1,02. 1,84. 2,07
ALB	0	0,45. 0,61. 0,84	4,74. 4,93. 6,83	7,42. 6,52. 12,41
CEBPA	0	0,24. 0,45. 0,69	3,02. 4,08. 5,36	3,42. 4,73. 5,24
NANOG	1,84. 1,89. 1,61	0,4. 0,38. 0,35	0,17. 0,12. 0,09	0. 0. 0

Table S6. Quantitative RT-PCR (*AFP*, *ALB*, *CEBPA* and *NANOG*) of mesoderm differentiation markers; mRNA levels were analysed on day 0 and weeks 1, 2 and 3 of DPPSC differentiation into bone-like cells (n=3). mRNA levels were normalised to the housekeeping gene *GAPDH* and compared with levels in human liver cDNAs.

Gene	Day 0	Week 1	Week 2	Week 3
GFAP	0	0,52. 1,24. 0,97	3,51. 4,43. 2,09	7,74. 6,71. 5,08
MBP	0	0,74. 0,93. 1,02	2,41. 2,87. 3,09	2,52. 3,05. 5,84
Sox 1	0	0,48. 0,91. 0,82	0,82. 1,22. 1,53	1,1. 1,51. 1,9
NANOG	1,84. 1,89. 1,61	0,21. 0,34. 0,35	0,07. 0,09. 0,11	0. 0. 0,001

Table S7. Quantitative RT-PCR (*GFAP*, *MBP*, *SOX1*, *NANOG*) of neurectoderm differentiation markers. mRNA levels were analysed on day 0 and weeks 1, 2 and 3 of DPPSC differentiation into bone-like cells (n=3). mRNA levels were normalised to the housekeeping gene *GAPDH* and compared with levels in human brain cDNAs.